SIAM REVIEW
Vol. 52, No. 1, pp. 57–86

Application of Standard and Refined Heat Balance Integral Methods to One-Dimensional Stefan Problems*

S. L. Mitchell†
T. G. Myers‡

Abstract. The work in this paper concerns the study of conventional and refined heat balance integral methods for a number of phase change problems. These include standard test problems, both with one and two phase changes, which have exact solutions that enable us to test the accuracy of the approximate solutions. We also consider situations where no analytical solution is available and compare these to numerical solutions. It is popular to use a quadratic profile as an approximation of the temperature, but we show that a cubic profile, seldom considered in the literature, is far more accurate in most circumstances. In addition, the refined integral method can give greater improvement still, and we develop a variation on this method which turns out to be optimal in some cases. We assess which integral method is better for various problems, showing that it is largely dependent on the specified boundary conditions.

Key words. heat balance integral method, phase change, Stefan problems

AMS subject classifications. 80A22, 40C10, 35K05

DOI. 10.1137/080733036

1. Introduction. The heat balance integral method (HBIM) is an approximate technique for solving thermal problems. It was originally proposed by Goodman [13, 14, 15] as an adaptation of the Karman–Pohlhausen integral method [37] for analyzing boundary layers; see [39] for a translated account of this work. Since exact solutions have been found for many problems in heat transfer, the HBIM has made its greatest impact on Stefan problems, where very few exact solutions can be found. Obviously other approximate solution techniques exist, such as numerical methods, perturbation solutions, and ray methods; see, for example, [1, 7, 8, 16, 18, 23, 26, 35]. Despite the fact that the HBIM may not always be as accurate as some of these methods, it remains a popular choice due to its simplicity and the fact that it produces analytic solutions for a wide range of problems and parameter values.

Consider a semi-infinite solid, initially at a constant temperature. The boundary $x = 0$ is suddenly heated to another constant temperature. The HBIM solution

*Received by the editors August 15, 2008; accepted for publication (in revised form) June 26, 2009; published electronically February 5, 2010.
http://www.siam.org/journals/sirev/52-1/73303.html

†Corresponding author. MACSI, Department of Mathematics and Statistics, University of Limerick, Limerick, Ireland (sarah.mitchell@ul.ie). This author was supported by the Mathematics Applications Consortium for Science and Industry (www.macsi.ul.ie) funded by Science Foundation Ireland Mathematics Initiative grant 06/MI/005.

‡Centre de Recerca Mathemàtica, UAB Science Faculty, Barcelona, Spain.

proceeds as follows:

1. First, introduce the heat penetration depth, $\delta(t)$. For $x \geq \delta$, the temperature rise is negligible.
2. Then define an approximate function for the temperature, typically a polynomial, and apply sufficient boundary conditions at $x = 0$ and $\delta(t)$ to determine all unknown coefficients in terms of the unknown function δ.
3. Finally, integrate the governing equation for $x \in [0, \delta]$ to produce what is termed the *heat balance integral*. Typically, this results in an ordinary differential equation (ODE) for δ.

Hence the initial partial differential equation (PDE) is reduced to a first order ODE, which may often be solved analytically. However, the approximation to the temperature only satisfies the heat balance integral, not the original governing equation. Thus, the governing equation will only be satisfied in an averaged or integral sense [2].

When solving a Stefan problem, the approach is similar except the position of the moving boundary is also unknown. The Stefan condition provides a further equation to determine this. Here the original problem consists of two PDEs in the two phases; the domain of these phases is unknown a priori and is defined by an ODE. Using the HBIM this reduces to solving two first order ODEs. In the idealized case of the melting of a solid initially at its solidus, the problem reduces to a first order ODE coupled with an algebraic equation.

The choice of approximating function is a constant source of debate [3, 21, 31]. Goodman primarily employed a quadratic. However, even for this simple choice Wood [43] shows six different formulations and demonstrates that Goodman's choice is typically third best, i.e., that it has the smallest error in the melt-front position $s(t)$. In fact, there is a seventh formulation; all these different methods will be discussed in section 3. The obvious next step is a cubic approximating function, and this is mentioned by Goodman [13]. Myers et al. [35] choose a cubic function when studying the melting of a subcooled finite block. Their choice is motivated by analyzing the melting of a material initially at its solidus. Both the small argument expansion of the exact solution and an asymptotic solution lead to a cubic with no quadratic term. They go on to show that this form is more accurate than a quadratic when analyzing the melting of a subcooled finite block. Antic and Hill [2] use two cubics to describe the temperature in grain and its surrounding air in a model of thermal diffusion in a grain store. Mitchell and Myers [24] employ a quartic in a study of ablation. This choice is motivated through an analysis of the heating-up stage before ablation commences. Their results are compared with an analysis of Braga, Mantelli, and Azevedo [4, 5], who use functions of the form

$$u = a_0 + a_1(\delta - x)^n. \tag{1.1}$$

Mosally, Wood, and Al-Fhaid [27] note that many thermal problems have exponentially decaying solutions, and consequently they use an exponential form. This performs well for the problem that motivated the choice; however, for the melting problem investigated in [35] it is the worst of the choices investigated. They also use piecewise linear and exponential approximations to improve the accuracy of the method. Mosally, Wood, and Al-Fhaid [28] investigate the convergence properties of the piecewise linear form and conclude that convergence is slow compared to that of finite difference schemes. We will discuss the single exponential method further in subsequent sections and describe cases where it is the best approximating function. A logical conclusion

of the HBIM is to look for a series solution. The generalized integral balance method involves a solution of the form

$$u = a_0 + \Sigma_{k=1}^{n} a_k(t) f_k(x), \tag{1.2}$$

where f_k form a linearly independent system and satisfy recurrence relations; see [41] (the method is described in [12]). Fomin, Chugunov, and Hashida [12] carry out calculations only up to $n = 2$ and describe the calculations as "tedious but straightforward." Since one of the main appeals of the HBIM is its simplicity, this may explain the lack of popularity of this generalization. A general introduction to the application of the HBIM to thermal problems and the choice of n is given in [17].

The majority of studies using the HBIM impose a fixed temperature at the substrate that is greater than the melt temperature, $U_0 > U_m$. This leads to immediate melting. When studying the melting of a subcooled material subject to a Robin condition, melting is not always immediate and this means there will be a premelting stage where a standard solution to the heat equation may be found and compared with the approximate solution. This approach is employed in [4, 5, 35], for example. In a series of papers, Braga, Mantelli, and Azevedo [4, 5] investigate ablation using the HBIM, which has a preablation stage. They choose the power n for the approximating function of (1.1) from matching the time to ablation predicted by an exact solution and by the HBIM. Once ablation starts they switch to a higher value, $m > n$. This approach suffers from two major drawbacks. First, the initial approximation only works when an exact solution is known and therefore is of little value. Second, Mitchell and Myers [24] have shown that when switching the order of the polynomial there is the restriction that $m \leq n$, otherwise mass will be added to the ablating material. They go on to demonstrate that a quartic provides a good approximation for all time.

In the following work we begin our analysis by looking at the standard problem of melting a semi-infinite solid that is initially at the solidus. In this context we describe the usual HBIMs and then introduce the refined integral method (RIM) [38]. With a constant temperature boundary condition, an analytical solution exists and this provides a test for the accuracy of the approximate solutions. With a Robin condition at the substrate we compare with numerical solutions. All these results are given in section 5. In addition, we also consider two time-dependent boundary conditions, both having exact solutions. This leads us to introduce an alternative refined integral method (ARIM), which in certain cases can show a further improvement for either a Robin or flux boundary condition. In section 6 we move on to the more realistic problem of melting a semi-infinite block that is initially below the melting temperature. This requires a modification of the refined and standard HBIMs. Again with the constant temperature boundary condition there is an analytical solution that we use to validate the approximate solutions. Up to this stage all solutions have involved immediate melting; when we investigate the Robin condition we must first analyze an initial heating-up phase before melting begins. In the final sections we briefly describe how to apply the methods to melting of a finite block, where melting can occur on two fronts, and ablation of a finite media. In general, when we provide numerical solutions we will be using parameter values appropriate to ice and water, since these data are most readily available. Perhaps the most well-studied example of the HBIM on ablation occurs in the context of heat shields on space vehicles (see [4, 5], for example), and we will use parameter values appropriate to Teflon.

2. Problem Description. Consider the problem of two-phase melting of a semi-infinite solid, as depicted in Figure 2.1. During the melting process the melt region

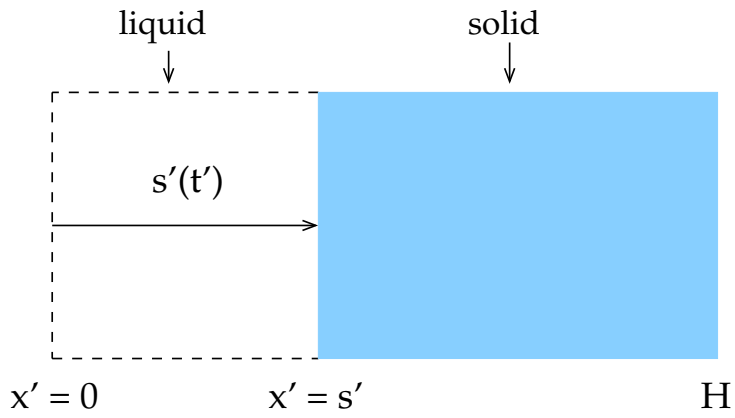

Fig. 2.1 *Schematic of a two-phase melting process.*

occupies $0 \leq x' \leq s'(t')$. If u' denotes the temperature in the melt and v' the temperature in the solid, then the problem is described by two heat equations,

$$\kappa_l \frac{\partial^2 u'}{\partial x'^2} = \frac{\partial u'}{\partial t'}, \qquad 0 < x' < s'(t'), \tag{2.1}$$

$$\kappa_s \frac{\partial^2 v'}{\partial x'^2} = \frac{\partial v'}{\partial t'}, \qquad x' > s'(t'), \tag{2.2}$$

where κ is the thermal diffusivity, subscripts l and s denote the liquid and solid, respectively, and primes indicate a dimensional quantity. Note that we assume the density remains constant during the phase change, i.e., $\rho_s = \rho_l = \rho$. This assumption is necessary to prevent an advection term from occurring in (2.1). The position of the interface is determined by the Stefan condition

$$\rho L_m \frac{\mathrm{d}s'}{\mathrm{d}t'} = k_s \frac{\partial v'}{\partial x'} - k_l \frac{\partial u'}{\partial x'} \qquad \text{at } x' = s', \tag{2.3}$$

where L_m is the latent heat of melting and k is the thermal conductivity. The boundary condition at $x' = s'$ is

$$u' = v' = U_m, \tag{2.4}$$

where U_m is the melting temperature. The initial condition is given by $v'(x', 0) = U_\infty$ ($U_\infty \leq U_m$), so either $v'_{x'} \to 0$ as $x' \to \infty$ or, equivalently, $v' \to U_\infty$. We consider the following two possible boundary conditions at $x' = 0$:

$$\text{(i)} \quad u' = U_0 \qquad \text{or} \qquad \text{(ii)} \quad k_l \frac{\partial u'}{\partial x'} = -Q + h_s(u' - U_0) \qquad \text{at } x' = 0, \tag{2.5}$$

where the source term Q could represent kinetic energy from an incoming fluid or aerodynamic heating, and h_s, for example, could be composed of thermal energy from an incoming fluid, evaporation, or convective heat transfer. These energy terms are discussed in more detail in [7, 32]. In section 6.2 we will discuss an initial premelting stage where h_s then represents the heat transfer coefficient between the solid and substrate. This is not necessarily the same as the liquid-substrate heat transfer

coefficient. The HBIM for boundary condition (i) is considered in [13, 27, 38, 43], but case (ii) with either $Q = 0$ or $h_s = 0$ is only briefly discussed in [13] and no comparisons are given with a numerical solution. Other investigations with $h_s = 0$ and Q constant are discussed in [4, 5, 15], whereas time-dependent boundary conditions are described in [4, 18, 45]. In the case of the convective boundary condition with $h_s \neq 0$, the HBIM has only been analyzed in [6, 46], while consideration with both $Q, h_s \neq 0$ is absent from the literature. In section 5.3 we briefly mention two test cases with time-dependent boundary conditions, one with $Q(t) \sim -e^t$ and the other with $u(0,t) \sim e^t - 1$. Both examples have the same exact solution, with the growth rate $s(t) \propto t$.

The problem can be rescaled by setting

$$x = \frac{x'}{L}, \qquad t = \frac{t'}{\tau}, \qquad u = \frac{u' - U_m}{U_0 - U_m}, \qquad v = \frac{v' - U_m}{U_m - U_\infty}, \qquad s = \frac{s'}{L}; \tag{2.6}$$

choosing a timescale of $\tau = L^2/\kappa_l$ means that the governing equations (2.1)–(2.5) become

$$\frac{\partial^2 u}{\partial x^2} = \frac{\partial u}{\partial t}, \qquad 0 < x < s, \tag{2.7}$$

$$\kappa \frac{\partial^2 v}{\partial x^2} = \frac{\partial v}{\partial t}, \qquad x > s, \tag{2.8}$$

$$\beta \frac{\mathrm{d}s}{\mathrm{d}t} = k\frac{\partial v}{\partial x} - \frac{\partial u}{\partial x} \qquad \text{at } x = s, \tag{2.9}$$

$$u = v = 0 \qquad \text{at } x = s, \qquad\qquad v = -1 \qquad \text{as } x \to \infty, \tag{2.10}$$

$$\text{(i)} \quad u = 1 \quad \text{or} \quad \text{(ii)} \quad \frac{\partial u}{\partial x} = -\gamma_1 + \gamma_2(u - 1) \qquad\qquad \text{at } x = 0, \tag{2.11}$$

with initial condition $v(x, 0) = -1$ and

$$\beta = \frac{\rho L_m \kappa_l}{k_l \Delta u} = \frac{1}{St}, \quad k = \frac{k_s}{k_l \Delta U}, \quad \kappa = \frac{\kappa_s}{\kappa_l}, \quad \gamma_1 = \frac{QL}{k_l \Delta u}, \quad \gamma_2 = \frac{h_s L}{k_l}, \tag{2.12}$$

where β is an inverse Stefan number, $\Delta u = U_0 - U_m$, $\Delta v = U_m - U_\infty$, and $\Delta U = \Delta u/\Delta v$. If we assume the thermal properties remain constant through the phase change, then we will obtain the more standard equations studied in [38, 27, 43, 8, 18]. However, for this study we retain the more general form.

In general, in the following work we will use parameter values appropriate to ice and water (which are relatively easy to obtain). These are displayed in Table 2.1. The value for the heat transfer coefficient, h_s, is of the order of magnitude of values quoted in [29, 32, 33, 35]. It should be noted that for the Robin boundary condition (2.11)(ii) melting will not occur immediately. There will be a premelting phase with the heat equation in the solid (2.8) holding for $x > 0$. The boundary condition (2.11)(ii) will hold for v instead of u at $x = 0$, but with the alteration

$$\frac{\partial v}{\partial x} = -\alpha_1 + \alpha_2(v - \Delta U), \qquad \text{where} \qquad \alpha_1 = \frac{QL}{k_s \Delta v}, \quad \alpha_2 = \frac{h_s L}{k_s}. \tag{2.13}$$

This is dealt with in section 6.2.

Table 2.1 *Physical parameter values for the liquid and solid.*

κ_l	1.35×10^{-7}	m^2/s	κ_s	1.16×10^{-6}	m^2/s
k_l	0.57	W/m K	k_s	2.18	W/m K
L_m	3.34×10^5	J/kg	h_s	180	$\mathrm{W/m}^2$ K
ρ	1000	$\mathrm{kg/m}^3$	U_0	278-373	K
U_m	273	K	U_∞	253	K

3. Melting of a Semi-infinite Material at the Solidus. We begin our analysis with the standard problem of the melting of a material initially at the solidus. Heat is applied at $x = 0$ so that melting occurs immediately. The system (2.7)–(2.10) reduces to

$$\frac{\partial^2 u}{\partial x^2} = \frac{\partial u}{\partial t}, \qquad 0 < x < s, \tag{3.1}$$

$$\beta \frac{\mathrm{d}s}{\mathrm{d}t} = -\frac{\partial u}{\partial x} \qquad \text{at } x = s, \tag{3.2}$$

$$u = 0 \qquad \text{at } x = s, \tag{3.3}$$

with the initial condition

$$u(x, 0) = 0 \qquad \text{for } x > 0. \tag{3.4}$$

Boundary conditions (2.11) are unchanged. If we apply (2.11)(i), then we may obtain an exact solution; with the Robin condition no analytical solution is known. We will investigate both possibilities.

The HBIM involves integrating the heat equation (3.1) with respect to x over the interval $(0, s(t))$. This gives

$$\left.\frac{\partial u}{\partial x}\right|_{x=s} - \left.\frac{\partial u}{\partial x}\right|_{x=0} = \frac{\mathrm{d}}{\mathrm{d}t}\int_0^s u \, \mathrm{d}x, \tag{3.5}$$

where, in deriving the integral term, we apply (3.3). Once an approximating function has been defined, (3.5) must be solved in conjunction with the Stefan condition (3.2). A variation on the method suggested by Goodman [13] comes from noting that $u(s(t), t) = 0$ for all t, hence the total derivative of the temperature at $x = s(t)$ is zero, i.e.,

$$\frac{\mathrm{D}u}{\mathrm{D}t}(s(t), t) = 0 \qquad \Longrightarrow \qquad \frac{\partial u}{\partial t} + \frac{\partial u}{\partial x}\frac{\mathrm{d}s}{\mathrm{d}t} = 0.$$

Then using (3.1) and (3.2) we can rewrite this as

$$\left(\frac{\partial u}{\partial x}\right)^2 = \beta \frac{\partial^2 u}{\partial x^2} \qquad \text{at } x = s. \tag{3.6}$$

This may be used as an alternative to the Stefan condition (3.2). To proceed further, a suitable approximating function must be defined for u. In the following sections we will first illustrate the method using the three most popular forms of approximating function, namely, quadratic, cubic, and exponential; see [13, 14, 15, 23, 24, 27, 35, 43], for example.

3.1. The Constant Temperature Boundary Condition. The exact solution to this problem is

$$u(x,t) = 1 - \frac{\operatorname{erf}\left[x/(2\sqrt{t})\right]}{\operatorname{erf}(\alpha)}, \qquad s(t) = 2\alpha\sqrt{t}, \tag{3.7}$$

where α satisfies the transcendental equation

$$\sqrt{\pi}\beta\alpha \operatorname{erf}(\alpha) e^{\alpha^2} = 1. \tag{3.8}$$

We will use this later to test the accuracy of the approximate solutions.

3.1.1. The Quadratic Profile. The original approximating function, proposed by Goodman [13, 14], is a quadratic of the form $u(x,t) = a(s-x) + b(s-x)^2$. However, Wood [43] favors the formulation

$$u(x,t) = a\left(1 - \frac{x}{s}\right) + b\left(1 - \frac{x}{s}\right)^2, \tag{3.9}$$

since this leads to coefficients a and b that are constant in time. In fact, this is only true when the boundary condition is of the form (2.11)(i). With a Robin condition they depend on time. Both formulations automatically satisfy the condition $u(s,t) = 0$. Applying $u(0,t) = 1$ gives $b = 1 - a$ and we are left with

$$u(x,t) = a\left(1 - \frac{x}{s}\right) + (1-a)\left(1 - \frac{x}{s}\right)^2. \tag{3.10}$$

Equation (3.10) shows that

$$\left.\frac{\partial u}{\partial x}\right|_{x=s} = -\frac{a}{s}, \qquad \left.\frac{\partial u}{\partial x}\right|_{x=0} = \frac{a-2}{s}, \qquad \int_0^s u \,\mathrm{d}x = \frac{s(a+2)}{6}, \tag{3.11}$$

while the Stefan condition (3.2) becomes

$$s\frac{\mathrm{d}s}{\mathrm{d}t} = \frac{a}{\beta}. \tag{3.12}$$

Since this comes from the linear term in the approximating function, the same condition will hold for the cubic approximation of the following section. The integral expression (3.5) may now be written

$$\left.\frac{\partial u}{\partial x}\right|_{x=s} - \frac{a-2}{s} = \frac{a+2}{6}\frac{\mathrm{d}s}{\mathrm{d}t}, \tag{3.13}$$

where the assumption that a is constant has been applied. The Stefan condition (3.2) may be used to replace the temperature gradient at $x = s$ in (3.13) to give a differential equation in terms of the two unknowns $s(t)$ and a,

$$s\frac{\mathrm{d}s}{\mathrm{d}t} = \frac{6(2-a)}{6\beta + a + 2}. \tag{3.14}$$

Equation (3.12) provides a second equation for these two unknowns. Combining these two expressions we find that the constant a satisfies the quadratic equation

$$a = -1 - 6\beta + \sqrt{1 + 24\beta + 36\beta^2}, \tag{3.15}$$

where we have used the positive square root to ensure $u_x(s,t) < 0$. Noting that a is a constant, then from either (3.12) or (3.14) it is clear that, as in the exact solution (3.7), $s \propto t^{1/2}$,

$$s(t) = 2\alpha\sqrt{t}, \qquad \alpha = \sqrt{\frac{a}{2\beta}}. \tag{3.16}$$

Now that a and $s(t)$ are known we can predict the evolution of the melt front, and by substituting these into (3.10) we also know the temperature $u(x,t)$ for all time.

The above method details one way to use the HBIM with a quadratic approximating function. However, Wood [43] shows that with this quadratic there are in fact six different formulations of the Stefan problem (3.1)–(3.3), each resulting in a different expression for a. These are found using permutations of the two forms of Stefan condition (3.6), (3.12) together with three ways of evaluating $u_x(s,t)$ in (3.13). So, instead of using (3.12) we may substitute u into (3.6) and find

$$a = -\beta + \sqrt{\beta^2 + 2\beta}. \tag{3.17}$$

The three ways of evaluating $u_x(s,t)$ are, first, by using (3.2) as above; second, by using (3.6) to find

$$\left.\frac{\partial u}{\partial x}\right|_{x=s} = -\sqrt{\beta \left.\frac{\partial^2 u}{\partial x^2}\right|_{x=s}} = -\frac{\sqrt{2\beta(1-a)}}{s}$$

(again we choose the appropriate root so $u_x(s,t) < 0$); and third, by using the first relation in (3.11). In each case the solution takes the form $s = 2\alpha\sqrt{t}$ with different expressions for α. Obviously there is some overlap in these permutations and so, of these six options, two sets are equivalent and there are only four distinct values for α in (3.16). The relative accuracy of each method depends on the value of β.

Goodman [13] considered two formulations, with the first corresponding to one of Wood's six options. Wood points out that for the majority of problems this formulation is in fact only the third best option. The second formulation described by Goodman, which is not discussed by Wood, involves neglecting the integral form (3.5) and instead combining the two forms of Stefan condition (3.12) and (3.17). This method therefore only satisfies the PDE (3.1) at $x = s$, but it is more accurate than all the other formulations for a small range of β ($2/15 < \beta < 3/8$).

The six methods described by Wood, and the seventh from Goodman, have a point of intersection in the plots of $\alpha(\beta)$ when $\beta = 2/15$. For melting ice this corresponds to a temperature scale $\Delta u \approx 544\,\mathrm{K}$, which is clearly not of practical interest. Given that for ice we are only likely to consider $\Delta u < 100\,\mathrm{K}$, using data from Table 2.1, this requires $\beta > 0.73$. In this case the method described above, leading to equations (3.15) and (3.16), is generally the most accurate.

3.1.2. The Cubic Profile. When considering the melting of a finite block, Myers et al. [35] employ a cubic profile, where the quadratic term is neglected. This form is based on both an asymptotic solution and the small argument expansion of an exact solution. Goodman [13] also mentioned the cubic profile, but then almost exclusively worked with a quadratic. Antic and Hill [2] employ two cubics in a double diffusion problem. In general we may work with a cubic including the quadratic term,

$$u(x,t) = a\left(1 - \frac{x}{s}\right) + b\left(1 - \frac{x}{s}\right)^2 + c\left(1 - \frac{x}{s}\right)^3, \tag{3.18}$$

where again a, b, and c are constant for the case of fixed temperature, $u(0,t) = 1$. This expression automatically satisfies $u(s,t) = 0$ and we require $c = 1 - a - b$ in order to satisfy $u(0,t) = 1$. There is now one more coefficient than in the quadratic case, and so we immediately use the alternative form of the Stefan condition (3.6) to give $b = \frac{a^2}{2\beta}$. Then (3.18) becomes

$$u(x,t) = a\left(1 - \frac{x}{s}\right) + \frac{a^2}{2\beta}\left(1 - \frac{x}{s}\right)^2 + \left(1 - a - \frac{a^2}{2\beta}\right)\left(1 - \frac{x}{s}\right)^3, \tag{3.19}$$

which now involves only one unknown coefficient a and the unknown melting front position $s(t)$. Even though we have used the alternative form of the Stefan condition, we must also use the original form (3.2), due to the extra coefficient. This means there can only be three possible formulations, which arise from the different ways of expressing $\frac{\partial u}{\partial x}\big|_{x=s}$. Following the same analysis as for the quadratic case, we find that the three possible forms all reduce to the same expression for a and so we only have one formulation here; this was noted in [13]. The unknown a for the cubic profile is found by substituting u from (3.19) into the heat balance integral (3.5) to give

$$s\frac{\mathrm{d}s}{\mathrm{d}t} = -\frac{12(a^2 + 6a\beta - 6\beta)}{a^2 + 6a\beta + 6\beta}. \tag{3.20}$$

Since a is constant, we will find $s \propto t^{1/2}$. The left-hand side is replaced by the as yet unused Stefan condition (3.2) (which reduces to the same expression as in the quadratic case, namely, (3.12)) and we obtain the following cubic expression for a:

$$a^3 + 18\beta a^2 + 6\beta(1 + 12\beta)a - 72\beta^2 = 0. \tag{3.21}$$

Once this has been determined numerically we may solve (3.12) to give the equation for $s(t)$ in (3.16), but with a now found from (3.21).

3.1.3. The Exponential Profile. The exponential profile proposed by Mosally, Wood, and Al-Fhaid [27] is motivated by the exact solution (3.8) and noting that the small z expansion of $\operatorname{erf} z \sim \frac{2}{\sqrt{\pi}} z\, e^{-z^2}$. Consequently, they take an approximating function of the form

$$u = a + \frac{bx}{s} e^{-cx^2/s^2}. \tag{3.22}$$

Imposing $u(s,t) = 0$ and $u(0,t) = 1$ leads to

$$u = 1 - \frac{x}{s} e^{c(1 - x^2/s^2)}. \tag{3.23}$$

Mosally, Wood, and Al-Fhaid [27] also propose an alternative exponential form, $u = a + be^{-cx/s}$, but this is never as accurate as (3.22) and is therefore not used here. Again we find there are six possible variations which reduce to four distinct solutions. The most accurate (for realistic β) is obtained following the first method detailed in section 3.1.1 giving the Stefan condition

$$s\frac{\mathrm{d}s}{\mathrm{d}t} = \frac{1 - 2c}{\beta}. \tag{3.24}$$

The solution to the system is

$$s(t) = 2\alpha\sqrt{t}, \qquad \alpha = \sqrt{\frac{1 - 2c}{2\beta}}, \tag{3.25}$$

where c satisfies the nonlinear relation

$$(1-2c)\big[2(1+\beta)ce^{-c}+e^{-c}-1\big]=2c\beta. \tag{3.26}$$

3.2. The Robin Boundary Condition. We now turn to the problem of solving the system (3.1)–(3.3) with the Robin condition (2.11)(ii) applied at $x=0$. Again we consider quadratic, cubic, and exponential approximating functions but to save time only discuss the best formulations (when compared to our subsequent numerical solution).

3.2.1. The Quadratic Profile. Assuming a temperature profile of the form (3.9) and applying the boundary condition (2.11)(ii) gives

$$u=a\left(1-\frac{x}{s}\right)+\left[\frac{(\gamma_1+\gamma_2)s-(1+\gamma_2 s)a}{2+\gamma_2 s}\right]\left(1-\frac{x}{s}\right)^2. \tag{3.27}$$

As in section 3.1.1 we substitute u directly into the integrated form of the heat equation (3.5) to find

$$\frac{2\big[(\gamma_1+\gamma_2)s-(1+\gamma_2 s)a\big]}{s(2+\gamma_2 s)}=\frac{\mathrm{d}}{\mathrm{d}t}\left[\frac{s\big[2(\gamma_1+\gamma_2)s+(4+\gamma_2 s)a\big]}{6(2+\gamma_2 s)}\right]. \tag{3.28}$$

This equation must be solved in conjunction with the Stefan condition (3.12). Note that we cannot assume a is constant in this case and so there are now two differential equations to solve for the unknowns $a(t)$ and $s(t)$. Since $s(0)=0$, it is clear that $a(0)=0$ to ensure that the initial condition $u(x,0)=0$ is satisfied in (3.27).

3.2.2. The Cubic Profile. The cubic form is defined by (3.18). After applying the boundary condition (2.11)(ii) and the alternative form of the Stefan condition (3.6), the temperature becomes

$$u(x,t)=a\left(1-\frac{x}{s}\right)+\frac{a^2}{2\beta}\left(1-\frac{x}{s}\right)^2+\left[\frac{(\gamma_1+\gamma_2)s-(1+\gamma_2 s)a-\frac{a^2}{2\beta}(2+\gamma_2 s)}{3+\gamma_2 s}\right]\left(1-\frac{x}{s}\right)^3. \tag{3.29}$$

Substituting this into (3.5) leads to

$$\begin{aligned}&\frac{\big[6\beta(\gamma_1+\gamma_2)s-6\beta(1+\gamma_2 s)a-a^2\gamma_2 s\big]}{2\beta s(3+\gamma_2 s)}\\&\quad=\frac{\mathrm{d}}{\mathrm{d}t}\left[\frac{s\big[6\beta(\gamma_1+\gamma_2)s+6\beta(5+\gamma_2 s)a+a^2(6+\gamma_2 s)\big]}{24\beta(3+\gamma_2 s)}\right].\end{aligned} \tag{3.30}$$

Coupling this to the Stefan condition (3.12) we obtain a pair of equations for $a(t)$ and $s(t)$. Again note that the initial condition for a is $a(0)=0$.

3.2.3. The Exponential Profile. Finally, we impose an exponential profile of the form (3.22). After applying (2.11)(ii) we find

$$u=\frac{(\gamma_1+\gamma_2)e^{-c}s}{1+\gamma_2 e^{-c}s}\left(1-\frac{x}{s}e^{c(1-x^2/s^2)}\right). \tag{3.31}$$

Substituting this into (3.5) leads to

$$\frac{(\gamma_1+\gamma_2)\big[1-e^{-c}(1-2c)\big]}{1+\gamma_2 e^{-c}s}=\frac{\mathrm{d}}{\mathrm{d}t}\left[\frac{(\gamma_1+\gamma_2)\big[-1+e^{-c}(1+2c)\big]s^2}{2c(1+\gamma_2 e^{-c}s)}\right]. \tag{3.32}$$

Calculating u_x and substituting it into the Stefan condition (3.2) gives

$$\frac{\mathrm{d}s}{\mathrm{d}t} = \frac{(\gamma_1+\gamma_2)e^{-c}(1-2c)}{\beta(1+\gamma_2 e^{-c}s)}. \tag{3.33}$$

To determine an initial condition for c we note that as $t \to 0$, $s \to 0$, the temperature $u \to 0$ and $u_x|_{x=0} \to -\gamma_1 - \gamma_2$. The Stefan condition (3.2) may then be written

$$-\beta\frac{\mathrm{d}s}{\mathrm{d}t} \to -\gamma_1 - \gamma_2. \tag{3.34}$$

Comparison of this with (3.33) shows that the appropriate initial condition for c is $c(0) = 0$. Unfortunately, solving (3.32)–(3.33) numerically gives singularities near $t = 0$, arising from differentiating the right-hand side of (3.32) to obtain an explicit expression for $\frac{\mathrm{d}c}{\mathrm{d}t}$. We therefore find it convenient to follow [13, 15] and introduce $\phi(t) = \int_0^s u\,\mathrm{d}x$, which is simply the term in square brackets in (3.32). Clearly $\phi(0) = 0$ and we are left with a pair of differential equations to solve for s and ϕ, since c can be written in terms of these unknown variables. The system is closed with the relation

$$-2c(1+\gamma_2 e^{-c}s)\phi = (\gamma_1+\gamma_2)\big[1-e^{-c}(2c+1)\big]s^2. \tag{3.35}$$

If we were to introduce $\phi(t)$ into the quadratic or cubic analyses we would be able to obtain an explicit relation for the unknown coefficient a in terms of ϕ and s. Unfortunately, this is not the case for c here and so we differentiate (3.35) with respect to t. This might seem unnecessary, as there are now three differential equations instead of two, but the larger system turns out to be easier to solve numerically.

4. The Refined Integral Method (RIM). Goodman's basic approach was to integrate the heat equation once, to give (3.5), and impose a quadratic profile to describe the temperature. Sadoun [38] advocates a second integration coupled to a quadratic profile. Integrating (3.1) twice with respect to x gives

$$\int_0^s \left(\int_0^x \frac{\partial u}{\partial t}\,\mathrm{d}\xi\right)\mathrm{d}x = \int_0^s \left(\frac{\partial u}{\partial x} - \left.\frac{\partial u}{\partial x}\right|_{x=0}\right)\mathrm{d}x = u\big|_{x=s} - u\big|_{x=0} - s\left.\frac{\partial u}{\partial x}\right|_{x=0}. \tag{4.1}$$

The first term on the right-hand side is zero since $u(s,t) = 0$, and the double integral on the left-hand side can be integrated once by parts and the dummy variable ξ replaced with x:

$$\int_0^s\int_0^x \frac{\partial u}{\partial t}\,\mathrm{d}\xi\,\mathrm{d}x = s\int_0^s \frac{\partial u}{\partial t}\,\mathrm{d}x - \int_0^s x\frac{\partial u}{\partial t}\,\mathrm{d}x = s\frac{\mathrm{d}}{\mathrm{d}t}\int_0^s u\,\mathrm{d}x - \frac{\mathrm{d}}{\mathrm{d}t}\int_0^s xu\,\mathrm{d}x.$$

Substituting this back into (4.1) leads to the integral form

$$s\frac{\mathrm{d}}{\mathrm{d}t}\int_0^s u\,\mathrm{d}x - \frac{\mathrm{d}}{\mathrm{d}t}\int_0^s xu\,\mathrm{d}x = -u\big|_{x=0} - s\left.\frac{\partial u}{\partial x}\right|_{x=0}. \tag{4.2}$$

Sadoun then combines this with the standard HBIM integral formulation (3.5) and the Stefan condition (3.2) to obtain

$$\frac{\mathrm{d}}{\mathrm{d}t}\int_0^s xu\,\mathrm{d}x = u\big|_{x=0} - \beta s\frac{\mathrm{d}s}{\mathrm{d}t}. \tag{4.3}$$

The integral expression (4.2) could of course be used directly, and it seems a more appropriate form when $\frac{\partial u}{\partial x}$ is prescribed at $x = 0$. We call this the alternative RIM (ARIM) and it is discussed in more detail in the results in section 5 below.

We will now illustrate the RIM on the constant boundary condition problem of the previous section, namely, we solve the system (3.1)–(3.4) with boundary condition (2.11)(i). The analysis for the Robin boundary condition is similar and so the details are not given; we merely quote final results in the results section. The function $\phi = \int_0^s u dx$ introduced in the previous section has an analogous form $\psi = \int_0^s xu dx$ in the RIM formulation.

4.1. The Quadratic Profile. We assume u has the form (3.10). Substituting it into the integral equation (4.3) leads to

$$\frac{\mathrm{d}}{\mathrm{d}t}\left[\frac{s^2(1+a)}{12}\right] = 1 - \beta s\frac{\mathrm{d}s}{\mathrm{d}t}. \tag{4.4}$$

Sadoun now defines $\sigma = s^2$ and combines the Stefan condition (3.12) with (4.4) to give a single equation for σ. However, this change of variable is not necessary since a is constant for the fixed boundary condition. This means we can write $s(t) = 2\alpha\sqrt{t}$, where

$$\alpha = \sqrt{\frac{a}{2\beta}}, \qquad a = \frac{1}{2}\Big[-(1+6\beta) + \sqrt{1+36\beta+36\beta^2}\Big]. \tag{4.5}$$

Note the difference between this form and that obtained from the standard analysis (3.15). Again we could write down another six formulations, but the solution given by (4.5) is the most accurate for realistic β.

4.2. The Cubic Profile. As for the standard HBIM analysis, there is only one formulation for the cubic profile and the temperature is defined by (3.19). We now apply the same analysis as for the quadratic profile above and substitute u into (4.3) and the Stefan condition (3.12) to give

$$\frac{\mathrm{d}}{\mathrm{d}t}\left[\frac{s^2(3\beta+7\beta a+a^2)}{60\beta}\right] = 1 - \beta s\frac{\mathrm{d}s}{\mathrm{d}t}, \qquad s\frac{\mathrm{d}s}{\mathrm{d}t} = \frac{a}{\beta}. \tag{4.6}$$

Again $s(t) = 2\alpha\sqrt{t}$, with $\alpha = \sqrt{\frac{a}{2\beta}}$, where a satisfies

$$a^3 + 7\beta a^2 + 3\beta(1+10\beta)a - 30\beta^2 = 0. \tag{4.7}$$

This is again different to the equation obtained from the standard analysis, (3.21).

4.3. The Exponential Profile. We now substitute the exponential profile (3.22) into (4.3) and the Stefan condition (3.12). Just as for the quadratic profile, we could write down seven formulations, but we simply give the one which is most accurate for realistic β. Then (3.25) holds but (3.26) is replaced by

$$(1-2c)\big[2\sqrt{c} + 2c^{3/2} - \sqrt{\pi}e^c\mathrm{erf}(\sqrt{c})\big] = 4\beta c^{5/2}. \tag{4.8}$$

5. Results. In this section we discuss the results for the constant temperature and Robin boundary conditions. In addition, we mention two other test cases, with time-dependent boundary conditions at $x = 0$, which are examined in the literature; see [8, 18], for example.

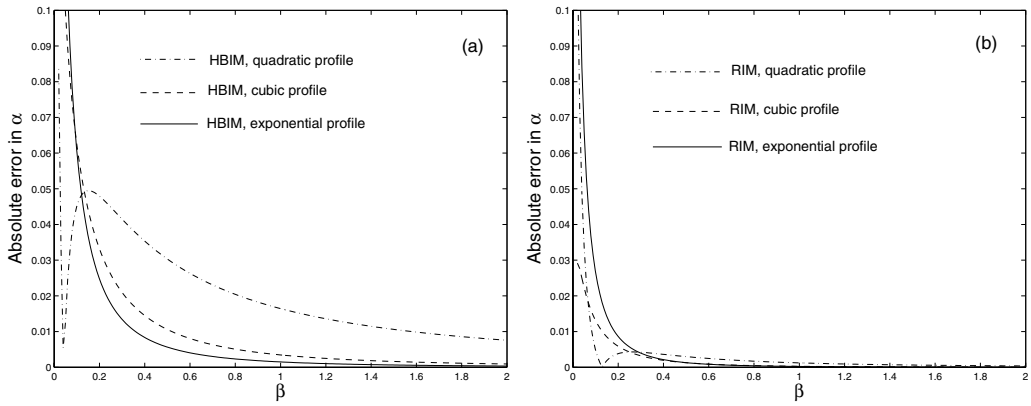

Fig. 5.1 *Plots of the absolute error in α against β for the three best methods, for HBIM in* (a) *and RIM in* (b)*, for boundary condition* (2.11)(i).

Table 5.1 *Comparison of infinity norm of the error in s (over $0 \le t \le 1$) between the numerical solution and the HBIM and RIM quadratic, cubic, and exponential profiles, for various $\beta \ge 1$, for the constant boundary condition.*

	HBIM			RIM		
β	Quadratic	Cubic	Exponential	Quadratic	Cubic	Exponential
1	3.3×10^{-2}	6.9×10^{-3}	3.0×10^{-3}	2.5×10^{-3}	5.4×10^{-4}	$\mathbf{4.5 \times 10^{-4}}$
1.25	2.6×10^{-2}	4.6×10^{-3}	1.9×10^{-3}	1.7×10^{-3}	3.1×10^{-4}	$\mathbf{2.4 \times 10^{-4}}$
$1.6\dot{7}$	1.9×10^{-2}	2.6×10^{-3}	1.0×10^{-3}	1.0×10^{-3}	1.4×10^{-4}	$\mathbf{1.1 \times 10^{-4}}$
2.5	1.1×10^{-2}	1.2×10^{-3}	4.1×10^{-4}	4.7×10^{-4}	4.8×10^{-5}	$\mathbf{3.1 \times 10^{-5}}$
5	4.6×10^{-3}	2.5×10^{-4}	8.2×10^{-5}	1.1×10^{-4}	5.3×10^{-6}	$\mathbf{3.4 \times 10^{-6}}$
10	1.7×10^{-3}	5.0×10^{-5}	1.5×10^{-5}	2.2×10^{-5}	5.4×10^{-7}	$\mathbf{3.3 \times 10^{-7}}$

5.1. The Constant Temperature Boundary Condition. In Figure 5.1 we present a comparison of the absolute error in the growth rate coefficient α for the various models against the inverse Stefan number β. We present the results in this way to enable comparison with [43], where similar plots are given to compare the six different quadratic formulations. It is clear that the RIM profiles shown on the right in (b) are all significantly more accurate than the HBIM profiles in (a). This was noted in [38], but there they considered only quadratic profiles for u. The cubic and exponential profiles in the RIM formulations show a great improvement and, although hard to see here, the latter is slightly more accurate as β increases. In both the figures it is clear that the quadratic approximation is best only over a very small parameter range.

As discussed in section 3.1.1 (for water at least), in practical applications it is realistic to assume $\beta > 0.7$. In Table 5.1 we therefore present the infinity norm of the error in s, over $0 \le t \le 1$, for larger values of β. The smallest errors are shown in bold. The conclusions are the same as for lower β but we present it in this form to enable comparisons with the results for the Robin boundary condition shown below, and it is easier to observe the errors for large β. For HBIM, the exponential and cubic approximations give errors an order of magnitude less than those obtained with the quadratic. The exponential is clearly the best, although the error is of the same order

Table 5.2 *Comparison of infinity norm of the error in s (over $0 \le t \le 1$) between the numerical solution and the HBIM and RIM quadratic, cubic, and exponential profiles, for various $\beta \ge 1$, for the Robin boundary condition.*

	HBIM			RIM		
β	Quadratic	Cubic	Exponential	Quadratic	Cubic	Exponential
1	7.8×10^{-3}	1.5×10^{-3}	1.1×10^{-2}	4.2×10^{-3}	$\mathbf{1.3 \times 10^{-3}}$	7.7×10^{-3}
1.25	5.5×10^{-3}	$\mathbf{8.6 \times 10^{-4}}$	8.3×10^{-3}	3.6×10^{-3}	9.0×10^{-4}	6.6×10^{-3}
$1.6\dot{7}$	3.4×10^{-3}	$\mathbf{3.8 \times 10^{-4}}$	5.4×10^{-3}	2.6×10^{-3}	4.7×10^{-4}	5.3×10^{-3}
2.5	1.5×10^{-3}	$\mathbf{1.0 \times 10^{-4}}$	2.7×10^{-3}	1.7×10^{-3}	1.6×10^{-4}	3.7×10^{-3}
5	3.0×10^{-4}	$\mathbf{6.0 \times 10^{-6}}$	5.8×10^{-4}	4.3×10^{-4}	2.3×10^{-4}	1.8×10^{-3}
10	4.2×10^{-5}	$\mathbf{2.0 \times 10^{-6}}$	5.0×10^{-4}	2.4×10^{-4}	2.9×10^{-4}	8.2×10^{-4}

as the cubic. When we move to RIM, there is an order of magnitude improvement for all approximating functions when compared to the standard method. Again the exponential is best, but the errors are very similar to those obtained by the cubic approximation. In fact, the correspondence here is much closer than with the HBIM. For the HBIM Mosally, Wood, and Al-Fhaid [27] pointed out that the exponential was the best method (when compared to the quadratic). However, this is no surprise since this approximating form was based on the exact solution. As we show in section 5.2 below, it does not necessarily provide the best approximation for different boundary conditions.

Before considering the Robin boundary condition we briefly return to discuss the accuracy of the HBIM for various values of the Stefan number β. For this test problem we can compare the predicted dependence of α on β with the exact solution. From the transcendental equation (3.8) it is clear that the exact solution has $\alpha \sim 1/\sqrt{2\beta}$ as $\beta \to \infty$. The HBIM/RIM profiles agree with this limit: for example, from (3.15) we find that $a/\beta \sim 1/\beta$ as $\beta \to \infty$, and combining with (3.16) gives the correct behavior. However, in the limit $\beta \to 0$, the exact solution (3.8) has $\alpha \sim \sqrt{\ln(1/\beta)}$ [1], but the HBIM/RIM profiles do not predict this dependence. Again using (3.15)–(3.16), it can be shown that as $\beta \to 0$, $a/\beta \sim 6$. This explains why the accuracy in Tables 5.1 and 5.2 significantly increases as β decreases, which can also be seen in Figure 5.1.

5.2. The Robin Boundary Condition. In Table 5.2 we present a comparison of results for the Robin boundary condition with $\gamma_1 = 0$, $\gamma_2 = 3.16$; these values come from applying the data in Table 2.1 to the definitions in (2.12) with $Q = 0$ and lengthscale $L = 1 \times 10^{-2}$m. Since there is no exact solution for this problem, we compare with L_∞ calculated using the numerical solution of [26]. Again the smallest error is shown in bold. Note that in this case (except for the largest value of β) the standard cubic HBIM provides the best approximation and is in fact often an order of magnitude more accurate than the exponential. For $\beta < 5$ the refined cubic has an error similar to the standard cubic and provides the best approximation for $\beta \le 1$.

5.3. Example with Growth Rate $\propto$ t. We now briefly discuss two related test cases for the single phase semi-infinite problem. Again we solve the system (3.1)–(3.4) but now look for a traveling wave solution in terms of the variable $\eta = x - ct$. The result is a solution of the form

$$u(x,t) = \beta\big(e^{-c(x-ct)} - 1\big), \qquad s(t) = ct. \tag{5.1}$$

Table 5.3 *Comparison of infinity norm of the error in s (over $0 \le t \le 1$) between the exact solution and the HBIM, RIM, and ARIM quadratic and cubic profiles, for boundary conditions* (5.2).

	HBIM		RIM		ARIM	
B.C.	Quadratic	Cubic	Quadratic	Cubic	Quadratic	Cubic
B.C. (5.2)(a)	2.4×10^{-2}	2.3×10^{-3}	4.4×10^{-3}	$\mathbf{2.9 \times 10^{-4}}$	4.4×10^{-2}	4.1×10^{-2}
B.C. (5.2)(b)	1.8×10^{-2}	$\mathbf{1.3 \times 10^{-3}}$	1.2×10^{-2}	2.8×10^{-3}	4.5×10^{-2}	2.5×10^{-3}

Table 5.4 *Comparison of infinity norm of the error in u (at $t = 1$) between the exact solution and the HBIM, RIM, and ARIM quadratic and cubic profiles, for boundary conditions* (5.2).

	HBIM		RIM		ARIM	
B.C.	Quadratic	Cubic	Quadratic	Cubic	Quadratic	Cubic
B.C. (5.2)(a)	1.9×10^{-2}	$\mathbf{3.5 \times 10^{-3}}$	3.3×10^{-2}	4.6×10^{-3}	2.2×10^{-2}	5.5×10^{-2}
B.C. (5.2)(b)	7.5×10^{-2}	9.9×10^{-3}	1.7×10^{-1}	2.8×10^{-2}	2.4×10^{-2}	$\mathbf{6.0 \times 10^{-3}}$

This was first found by Stefan; see [9, p. 292]. The stability of the solution and its application to combustion theory is discussed in [36]. Consequently, we can look for solutions using the approximate method subject to the following time-dependent boundary conditions at $x = 0$:

$$\text{(5.2)} \qquad \text{(a)} \quad u(0,t) = \beta\big(e^{c^2 t} - 1\big), \qquad \text{(b)} \quad \left.\frac{\partial u}{\partial x}\right|_{x=0} = -\beta c e^{c^2 t}.$$

Caldwell and Kwan [8] consider the former and Kutluay, Bahadir, and Ozdes [18] consider the latter, both with $\beta = c = 1$.

The integral method analysis is not presented here as it is identical to that described above for the constant and Robin boundary conditions (2.11). Also, we consider only the quadratic and cubic profiles since the ODEs for the exponential profile are more complicated to solve numerically and lead to less accurate results, as found for the Robin boundary condition.

In Table 5.3 we present the L_∞ norm error for $\beta = 1$. It is clear that β can be scaled out of the problem by setting $u = \beta\hat{u}$, and so these errors are independent of β. They show that when u is prescribed on the boundary $x = 0$, the cubic RIM is the most accurate method. However, when $\frac{\partial u}{\partial x}$ is defined instead, the cubic HBIM is more accurate. This makes sense because here we know $\frac{\partial u}{\partial x}$ at $x = 0$ exactly. As can be seen from the derivation in section 4.1, the RIM removes this term using the standard HBIM formulation, and it seems likely that this will introduce more error. The last two columns in Table 5.3 shows the errors for ARIM, which uses (4.2) directly. Unfortunately, neither the quadratic nor the cubic profile gives an improvement on the HBIM or RIM errors for s. However, in Table 5.4 we examine the infinity norm of the errors in the temperature u at $t = 1$; here the alternative RIM formulation is the most accurate for (5.2)(b). This shows that it can be important to examine the errors in u as well as in s. In addition, we conclude that the ARIM does not give any improvement in either s or u when u is prescribed at the $x = 0$ boundary and so, henceforth, we consider only ARIM when we have $\frac{\partial u}{\partial x}$ given there.

It should be noted that we could have considered the ARIM formulation for the Robin boundary condition (2.11)(ii). As for boundary condition (5.2)(b), we do not

see an improvement in the errors in s, but for $\beta \in (1.5, 7)$ the ARIM does give the smallest errors in u.

6. Melting of a Subcooled Semi-infinite Media.

6.1. The Constant Temperature Boundary Condition. We now consider the problem specified by the system (2.7)–(2.10), (2.11)(i). This has the exact solution

$$u = 1 - \frac{\operatorname{erf}\left(\frac{x}{2\sqrt{t}}\right)}{\operatorname{erf}\alpha}, \quad 0 < x < s, \qquad v = -1 + \frac{\operatorname{erfc}\left(\frac{x}{2\sqrt{\kappa t}}\right)}{\operatorname{erfc}(\alpha/\sqrt{\kappa})}, \quad s < x < \infty, \tag{6.1}$$

with interface height (see [10]) given by $s(t) = 2\alpha\sqrt{t}$ and α determined using the Stefan condition (2.9),

$$-\beta\alpha\sqrt{\pi} = -\frac{e^{-\alpha^2}}{\operatorname{erf}\alpha} + \frac{k}{\sqrt{\kappa}}\frac{e^{-\alpha^2/\kappa}}{\operatorname{erfc}(\alpha/\sqrt{\kappa})}. \tag{6.2}$$

For the subcooled block there is a quantitative difference from the formulation of the previous problems. When the solid is at the phase change temperature the problem reduces to solving for the position of the melt front. With a subcooled block there is a thermal boundary layer within the solid whose width must also be determined. So, to employ the HBIM it is standard to introduce the heat penetration depth, δ, which defines the width of the thermal boundary layer. We expect the boundary layer to merge smoothly with the region where $v = -1$ and therefore define the edge of the boundary layer with the conditions

$$v\big|_{x=\delta} = -1, \qquad \left.\frac{\partial v}{\partial x}\right|_{x=\delta} = 0. \tag{6.3}$$

The introduction of $\delta(t)$ is key to solving the semi-infinite problem as we now have a finite region $s(t) < x < \delta(t)$ where we can apply the HBIM and RIM. The quantity $\delta(t)$ is unknown but has initial condition $\delta(0) = 0$ and is determined as part of the solution process.

Applying the standard HBIM to both phases gives

$$\left.\frac{\partial u}{\partial x}\right|_{x=s} - \left.\frac{\partial u}{\partial x}\right|_{x=0} = \frac{\mathrm{d}}{\mathrm{d}t}\int_0^s u\,\mathrm{d}x, \qquad -\kappa\left.\frac{\partial v}{\partial x}\right|_{x=s} = \frac{\mathrm{d}}{\mathrm{d}t}\int_s^\delta v\,\mathrm{d}x + \frac{\mathrm{d}\delta}{\mathrm{d}t}. \tag{6.4}$$

For the RIM we perform a similar analysis to that described in section 4. A double integration of the PDE (2.7) for the liquid with respect to x over $0 < x < s(t)$ gives

$$\frac{\mathrm{d}}{\mathrm{d}t}\int_0^s xu\,\mathrm{d}x = u\big|_{x=0} + s\left.\frac{\partial u}{\partial x}\right|_{x=s}. \tag{6.5}$$

Note that this is identical to (4.3) except that we have not replaced $\frac{\partial u}{\partial x}\big|_{x=s}$ using the Stefan condition (2.9) (this avoids coupling of the u and v expressions, since the Stefan condition now involves $\frac{\partial v}{\partial x}\big|_{x=s}$).

In the solid region, a double integration for the corresponding PDE in (2.7) with respect to x over the region $s(t) < x < \delta(t)$ leads to

$$\int_s^\delta \left(\int_x^\delta \frac{\partial v}{\partial t}\,\mathrm{d}\xi\right)\mathrm{d}x = \kappa\int_s^\delta \left(\left.\frac{\partial v}{\partial x}\right|_{x=\delta} - \frac{\partial v}{\partial x}\right)\mathrm{d}x = -\kappa\Big[v\big|_{x=\delta} - v\big|_{x=s}\Big] = \kappa.$$

The left-hand side may be integrated by parts; after applying (6.4)(b), we obtain

$$\frac{\mathrm{d}}{\mathrm{d}t}\int_s^\delta xv\,\mathrm{d}x + \delta\frac{\mathrm{d}\delta}{\mathrm{d}t} = \kappa\left[1 - s\frac{\partial v}{\partial x}\bigg|_{x=s}\right]. \tag{6.6}$$

The ARIM formulation is not given here as the fixed temperature condition $u = 1$ is prescribed at $x = 0$.

At this stage we have even more choice for the approximating function, now we may expand in terms of $(1 - x/s)$ or $(1 - x/\delta)$. Since the melt region is defined for $x \in [0, s]$, we choose the former here. In the solid we choose the latter (in fact, after applying the boundary conditions we find that the two formulations are identical). However, the latter provides a more convenient form (it is also consistent with the expansion used in [24]). In the quadratic case, after applying the boundary conditions $u(0,t) = 1$, $u(s,t) = v(s,t) = 0$, and (6.3), these become

$$u = a\left(1 - \frac{x}{s}\right) + (1-a)\left(1 - \frac{x}{s}\right)^2, \quad 0 \le x \le s, \qquad v = -1 + \frac{(\delta - x)^2}{(\delta - s)^2}, \quad s \le x \le \delta.$$

We have three unknowns, namely, a, s, and δ, which are determined using the Stefan condition (2.9) coupled with either the HBIM (6.4) or RIM (6.5)–(6.6) formulations.

Substituting u and v into the Stefan condition (2.9) gives

$$\beta\frac{\mathrm{d}s}{\mathrm{d}t} = \frac{2k}{s - \delta} + \frac{a}{s}. \tag{6.7}$$

This admits a solution of the form

$$s(t) = 2\alpha\sqrt{t}, \qquad \delta(t) = 2\lambda\sqrt{t}, \tag{6.8}$$

for constant a. Substitution into the HBIM formulation (6.4) with Stefan condition (6.7) gives the following three equations to be solved for α, λ, and a:

$$\alpha^2 = \frac{6(1-a)}{2+a}, \qquad \lambda + 2\alpha = \frac{3\kappa}{\lambda - \alpha}, \qquad 2\alpha^2\beta = a - \frac{2\alpha k}{\lambda - \alpha}. \tag{6.9}$$

Alternatively, substitution into the RIM formulation (6.5)–(6.6) leads to

$$\alpha^2 = \frac{3(1-a)}{1+a}, \qquad 3\alpha^2 + 2\alpha\lambda + \lambda^2 = 3\kappa\left(\frac{\lambda + \alpha}{\lambda - \alpha}\right), \tag{6.10}$$

with the Stefan condition satisfying the third relation in (6.9), and we again solve for α, λ, and a.

When imposing a cubic approximation, further boundary conditions are required. In the melt region the alternative Stefan condition obtained from taking the total derivative of $u(s(t), t) = 0$ with respect to time is

$$\beta\frac{\partial^2 u}{\partial x^2} = \left(\frac{\partial u}{\partial x}\right)^2 - k\frac{\partial u}{\partial x}\frac{\partial v}{\partial x}, \tag{6.11}$$

which holds at $x = s$. We may obtain a similar condition from differentiating $v(s(t), t) = 0$; however, instead we apply the method to $v(\delta(t), t) = -1$ to obtain

$$\frac{\partial v}{\partial x}\frac{\partial \delta}{\partial t} + \frac{\partial v}{\partial t} = 0 \qquad \Longrightarrow \qquad \frac{\partial^2 v}{\partial x^2}\bigg|_{x=\delta} = 0, \tag{6.12}$$

where we have imposed $v_x(\delta, t) = 0$ and $\kappa v_{xx} = v_t$. The appropriate cubic profiles are

$$u = a\left(1 - \frac{x}{s}\right) + b\left(1 - \frac{x}{s}\right)^2 + (1 - a - b)\left(1 - \frac{x}{s}\right)^3, \qquad 0 \le x \le s, \tag{6.13}$$

$$v = -1 + \frac{(\delta - x)^3}{(\delta - s)^3}, \qquad s \le x \le \delta. \tag{6.14}$$

Substituting u and v from (6.13) and (6.14) into (6.11) gives

$$2\beta b = a^2 - \frac{3aks}{\delta - s}. \tag{6.15}$$

This allows us to eliminate b and we are left with the three unknowns, namely, a, δ, and s (as for the quadratic profile). Applying either the HBIM or RIM to u and v, and setting s and δ according to (6.8), leads to two algebraic equations, namely,

$$\text{HBIM:} \quad \alpha^2(3 + 3a + b) = 6(3 - 3a - b), \qquad 3\alpha + \lambda = \frac{6\kappa}{\lambda - \alpha};$$

$$\text{RIM:} \quad \alpha^2(3 + 7a + 2b) = 15(1 - a), \qquad 6\alpha^2 + 3\alpha\lambda + \lambda^2 = -\frac{5\kappa(\lambda + 2\alpha)}{\alpha - \lambda}.$$

In both cases the Stefan condition in (6.9) gives the third equation, and so these can be solved to determine α, λ, and a (since b is found from (6.15)).

In Tables 6.1 and 6.2 we present the absolute percentage error in α predicted by the exact solution and the approximate methods. Table 6.1 has results for a solid initially at temperature $U_\infty = 253$K (and so $\Delta v = 20$) and on a substrate with temperature varying from 278–373K. The smallest error is in bold font. In this case, for $\beta < 2$ the cubic HBIM is the most accurate. For $\beta > 2$ (except for one case) the

Table 6.1 *Comparison of percentage errors in α when $\Delta v = 20$.*

	HBIM		RIM	
Δu, β	Quadratic	Cubic	Quadratic	Cubic
100, 0.73	3.13	**0.21**	1.02	0.77
50, 1.45	1.89	**0.52**	0.88	1.60
35, 2.07	1.36	0.94	**0.79**	2.18
25, 2.90	0.92	1.29	**0.68**	2.84
15, 4.84	**0.37**	1.88	0.48	4.03
5, 14.52	0.54	3.46	**0.18**	7.38

Table 6.2 *Comparison of percentage errors in α when $\Delta v = 5$.*

	HBIM		RIM	
Δu, β	Quadratic	Cubic	Quadratic	Cubic
100, 0.73	3.18	0.52	0.69	**0.34**
50, 1.45	2.06	0.23	0.22	**0.13**
35, 2.07	1.57	**0.08**	0.17	0.19
25, 2.90	1.19	**0.03**	0.14	0.27
15, 4.84	0.75	0.15	**0.11**	0.4
5, 14.52	0.21	0.38	**0.04**	0.83

quadratic RIM is most accurate. The best quadratic HBIM is only most accurate for a single example. When the initial temperature is increased to $U_\infty = 271$K (i.e., $\Delta v = 2$), shown in Table 6.2, the quadratic HBIM is never most accurate. For large β the quadratic RIM is best; for intermediate values it is the cubic HBIM; and finally the cubic RIM is best for small values.

6.2. The Robin Boundary Condition. We will now briefly describe the melting process subject to a Robin condition. This process is qualitatively different to those discussed previously in that melting does not occur immediately and so we must first analyze a premelting phase, where there is only a solid region, which means that (2.8) is solved for $x > 0$ with boundary conditions (2.13) and $v = -1$ as $x \to \infty$ from (2.10). The cubic profile has, in general, proved the most accurate so far. Furthermore, as shown in [35], which analyzes the standard HBIM formulation for the melting of a finite block, the cubic profile is more accurate than the quadratic in the premelting phase when compared to the exact solution. Consequently, we now give the derivation only for the cubic profile but will show the quadratic results later.

Therefore, before melting begins we consider the cubic temperature profile

$$v = -1 + a\left(1 - \frac{x}{\delta}\right) + b\left(1 - \frac{x}{\delta}\right)^2 + c\left(1 - \frac{x}{\delta}\right)^3. \tag{6.16}$$

Since there is no melting we cannot impose the alternative Stefan condition; however, the total derivative of the constant temperature condition $v(\delta, t) = -1$ gives

$$\frac{\partial v}{\partial x}\frac{\partial \delta}{\partial t} + \frac{\partial v}{\partial t} = 0. \tag{6.17}$$

Substituting for v_t from the heat equation and imposing $v_x = 0$ shows $v_{xx}(\delta, t) = 0$. The temperature profile then reduces to the much simpler form

$$v = -1 + c\left(1 - \frac{x}{\delta}\right)^3. \tag{6.18}$$

The boundary condition (2.13) at $x = 0$ determines $c = \delta\big[\alpha_1 + \alpha_2(1+\Delta U)\big]/(3+\alpha_2\delta)$. The HBIM, RIM, and ARIM formulations are derived in the same way as discussed earlier, but now the heat equation (2.8) is integrated with respect to x over the interval $(0, \delta(t))$. This leads to expressions

$$\frac{\mathrm{d}}{\mathrm{d}t}\int_0^\delta v\,\mathrm{d}x + \frac{\mathrm{d}\delta}{\mathrm{d}t} = -\kappa\frac{\partial v}{\partial x}\bigg|_{x=0},$$

$$\delta\frac{\mathrm{d}}{\mathrm{d}t}\int_0^\delta v\,\mathrm{d}x - \frac{\mathrm{d}}{\mathrm{d}t}\int_0^\delta xv\,\mathrm{d}x = -\kappa\Big(1 + v\big|_{x=0}\Big) - \kappa\delta\frac{\partial v}{\partial x}\bigg|_{x=0}$$

for the HBIM and ARIM, respectively, with the RIM found by combining the two. Substituting v into these expressions gives

(6.19)

$$\text{HBIM: } \frac{\mathrm{d}}{\mathrm{d}t}(c\delta) = \frac{12\kappa c}{\delta}, \quad \text{RIM: } \frac{\mathrm{d}}{\mathrm{d}t}(c\delta^2) = 20\kappa c, \quad \text{ARIM: } 5\delta\frac{\mathrm{d}}{\mathrm{d}t}(c\delta) - \frac{\mathrm{d}}{\mathrm{d}t}(c\delta^2) = 40\kappa c.$$

These have the following implicit solutions:

$$\text{HBIM:}\quad \frac{1}{2}\alpha_2^2\delta^2 + 3\alpha_2\delta - 9\ln\left[3+\alpha_2\delta\right] = 12\alpha_2^2\kappa t - 9\ln 3; \tag{6.20}$$

$$\text{RIM:}\quad \alpha_2^2\delta^2 + 3\alpha_2\delta - 9\ln\left[3+\alpha_2\delta\right] = 20\alpha_2^2\kappa t - 9\ln 3; \tag{6.21}$$

$$\text{ARIM:}\quad \frac{1}{2}\alpha_2^2\delta^2 + 4\alpha_2\delta - 12\ln\left[3+\alpha_2\delta\right] = \frac{40}{3}\alpha_2^2\kappa t - 12\ln 3. \tag{6.22}$$

Melting begins at time t_m when $v(0,t_m)=0$. From (6.18) we see that this requires $c=1$ or $\delta = 3/(\alpha_1+\alpha_2\Delta U)$. Substituting this value of δ into (6.20)–(6.21) then gives the HBIM, RIM, and ARIM predictions of t_m.

The exact solution of this premelting problem is

$$v(x,t) = -1 + \frac{\alpha_1+\alpha_2(1+\Delta U)}{\alpha_2}\left[\operatorname{erfc}\left(\frac{x}{2\sqrt{\kappa t}}\right) - e^{\alpha_2 x+\alpha_2^2\kappa t}\operatorname{erfc}\left(\frac{x}{2\sqrt{\kappa t}}+\alpha_2\sqrt{\kappa t}\right)\right], \tag{6.23}$$

and so the exact value of t_m is the solution of

$$\alpha_2 = \left[\alpha_1+\alpha_2(1+\Delta U)\right]\left[1 - e^{\alpha_2^2\kappa t_m}\operatorname{erfc}\left(\alpha_2\sqrt{\kappa t_m}\right)\right]. \tag{6.24}$$

In this premelting phase, if $Q=0$ and $L = 1\times 10^{-2}$m, then using the definitions in (2.12) and parameter values in Table 2.1 we have $\alpha_1 = 0$, $\alpha_2 = 0.83$, and $\kappa \approx 8.59$. Tables 6.3 and 6.4 show the percentage errors in t_m for the quadratic profiles corresponding to HBIM, RIM, and ARIM. Two values of U_∞ are shown, and we see remarkably different results. In Table 6.3, the cubic ARIM is only best for very large Δu, and then the cubic HBIM becomes the most accurate (although this changes again when $\Delta u < \Delta v$). The quadratic HBIM and RIM lead to unacceptably large errors and should be avoided (except for $\Delta u < 5$, where the HBIM is most accurate). However, when Δv is very small, as shown in Table 6.4, the cubic ARIM is best in all but one case. Although not given here, the errors in u at $t = t_m/2$ also show that the cubic ARIM can be the most accurate for some values of Δu when $U_\infty = 253$, but this is not generally the case as Δv decreases. Again the quadratic HBIM and RIM solutions give large errors, whereas the cubic results are better in all cases.

Table 6.3 *Comparison of percentage error in t_m for the HBIM, RIM, and ARIM quadratic and cubic profiles when $\Delta v = 20$.*

	HBIM		RIM		ARIM	
Δu, β	Quadratic	Cubic	Quadratic	Cubic	Quadratic	Cubic
100, 0.73	13.6	2.8	33.9	10.7	6.7	**1.2**
50, 1.45	12.3	**1.3**	31.7	7.7	7.2	1.9
35, 2.07	11.2	**0.13**	30.0	5.5	7.5	2.5
25, 2.90	10.0	**1.2**	28.0	2.7	7.9	3.2
15, 4.84	7.7	3.9	24.0	**2.6**	8.6	4.5
5, 14.52	**1.6**	10.7	12.9	17.6	9.8	7.3

In the melting phase we solve (2.7)–(2.11)(ii) for $t > t_m$. The analysis is similar to that described in section 6.1 and we again introduce the heat penetration depth $\delta(t)$. Here we have $s(t_m) = 0$, with $v(x,t_m)$ and $\delta(t_m) = \delta_m$ taken from the premelting phase. Given the errors in t_m for the premelting phase, we consider only the cubic

Table 6.4 *Comparison of percentage error in t_m for the HBIM, RIM, and ARIM quadratic and cubic profiles when $\Delta v = 5$.*

	HBIM		RIM		ARIM	
Δu, β	Quadratic	Cubic	Quadratic	Cubic	Quadratic	Cubic
100, 0.73	14.7	4.1	35.7	13.2	6.3	**0.51**
50, 1.45	14.3	3.6	35.1	12.3	6.4	**0.73**
35, 2.07	14.0	3.3	34.5	11.6	6.5	**0.92**
25, 2.90	13.6	2.8	33.9	10.7	6.7	**1.2**
15, 4.84	12.7	1.8	32.4	8.7	7.0	**1.7**
5, 14.52	9.1	2.3	26.4	**0.57**	8.2	3.8

profiles. Therefore, the solution profile in the solid phase is again given by (6.14). However, instead of (6.13) we now have

(6.25)
$$u = a\left(1-\frac{x}{s}\right) + b\left(1-\frac{x}{s}\right)^2 + \left[\frac{(\gamma_1+\gamma_2)s - a(1+\gamma_2 s) - b(2+\gamma_2 s)}{3+\gamma_2 s}\right]\left(1-\frac{x}{s}\right)^3.$$

This is similar to (3.29) but b here is determined from the alternative Stefan condition (6.11), which also reduces to (6.15). Hence, b can be eliminated and we are left with three unknowns a, δ, and s. The Stefan condition again satisfies (6.7), but we now cannot assume s and δ are of the form (6.8) since a is not constant.

The HBIM (6.4) and RIM (6.5)–(6.6) formulations, respectively, give the following pair of ODEs:

$$\text{(6.26)}\quad \frac{\mathrm{d}\phi}{\mathrm{d}t} = \frac{-\gamma_2 bs + 3(\gamma_1+\gamma_2)s - 3a(1+\gamma_2 s)}{s(3+\gamma_2 s)}, \qquad \frac{\mathrm{d}\delta}{\mathrm{d}t} + 3\frac{\mathrm{d}s}{\mathrm{d}t} = \frac{12\kappa}{\delta - s},$$

$$\text{(6.27)}\quad \frac{\mathrm{d}\psi}{\mathrm{d}t} = \frac{b + (\gamma_1+\gamma_2)s - a(1+\gamma_2 s)}{3+\gamma_2 s}, \qquad \frac{\mathrm{d}}{\mathrm{d}t}\left[6s^2 + 3\delta s + \delta^2\right] = \frac{20\kappa(\delta+2s)}{\delta - s},$$

where $\phi = \int_0^s u\,\mathrm{d}x$ and $\psi = \int_0^s xu\,\mathrm{d}x$ are given by

$$\text{(6.28)}\qquad \phi = \frac{s\left[b(6+\gamma_2 s) + 3(\gamma_1+\gamma_2)s + 3a(5+\gamma_2 s)\right]}{12(3+\gamma_2 s)},$$

$$\text{(6.29)}\qquad \psi = \frac{s^2\left[b(9+2\gamma_2 s) + 3(\gamma_1+\gamma_2)s + a(27+7\gamma_2 s)\right]}{60(3+\gamma_2 s)}.$$

These can be used to determine an explicit expression for a in terms of s: we eliminate b using (6.15) and solve the resulting quadratic equations for a. The ARIM formulation can be derived in a similar manner. We find that

(6.30)
$$s\frac{\mathrm{d}\phi}{\mathrm{d}t} - \frac{\mathrm{d}\psi}{\mathrm{d}t} = \frac{-(1+\gamma_2 s)b + 2(\gamma_1+\gamma_2)s - 2a(1+\gamma_2 s)}{3+\gamma_2 s} \equiv R, \qquad 2\frac{\mathrm{d}\delta}{\mathrm{d}t} + 3\frac{\mathrm{d}s}{\mathrm{d}t} = \frac{20\kappa}{\delta - s}.$$

It is beneficial to define $\theta = s\phi - \psi$ and then the first ODE in (6.30) reduces to $\frac{\mathrm{d}\theta}{\mathrm{d}t} = \phi\frac{\mathrm{d}s}{\mathrm{d}t} + R$. The pair of ODEs in (6.26)–(6.27), (6.30) are combined with the Stefan condition (6.7) to solve for (s,δ,ϕ), (s,δ,ψ), or (s,δ,θ) for the HBIM, RIM, and ARIM, respectively. The functions ϕ and ψ have been introduced here for convenience; in two phase problems with a Robin boundary condition at $x = 0$, the resulting ODE systems

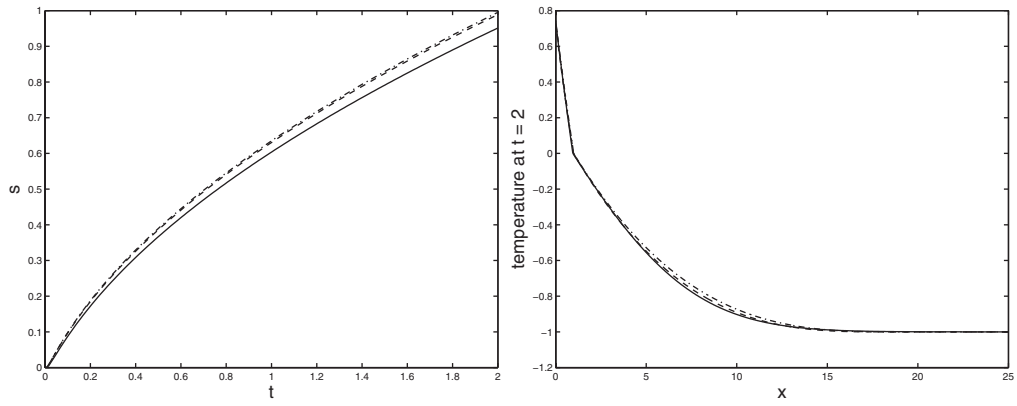

Fig. 6.1 *Melting phase for the Robin condition: the first plot shows the melt depth $s(t)$ and the second plot shows the temperatures u and v at $t = 1$. The solid line is the numerical solution, and HBIM and RIM are given by dotted and dashed lines, respectively.*

turn out to be easier to solve. We do not have to determine an initial condition for a but simply use $\phi(t_m) = \psi(t_m) = 0$.

There is no exact solution in the melting phase and so we must compare these heat balance methods to a numerical solution of the full problem. Vynnycky, Mitchell, and Aberg [42] study the numerical solution of one-dimensional time-dependent solidification, with focus on the continuous casting of copper. In that application there exist presolidification and solidification phases and so their numerical solution can be applied here in a similar manner. This is an extension of the numerical method described in [26], which considers numerical solutions of the classic single phase Stefan problem.

In Figure 6.1 we have plotted $s(t)$ against t and the temperature u and v at time $t = 1$. Parameter values used are $\Delta u = 35$ and $\Delta v = 20$, which give $k = 2.19$ and $\beta = 2.08$, with $\gamma_1 = 0$ and $\gamma_2 = 3.16$. We have not included the ARIM as it is indistinguishable from the RIM. The percentage errors in s at $t = 1$ are 2.2%, 4.4%, and 4.7% for the HBIM, RIM, and ARIM solutions, respectively. Therefore, the HBIM solution gives a more accurate prediction of $s(t)$ here; this is to be expected, since for these values it gave the most accurate prediction of t_m in the premelting phase, as can be seen in Table 6.3. However, the right-hand plot in Figure 6.1 shows that the RIM solution is noticeably more accurate in its prediction of v.

7. Extensions and Further Applications.

7.1. Ablation. Ablation is the process whereby mass is removed from an object by vaporization or other similar erosive processes. Perhaps the classic example involves the burning up of meteorites or heat shields on space vehicles. On space vehicles the exposed surface of the ablative material is designed to burn off and the resultant gases will carry much of the heat away, while the remaining material acts as an insulator. The process may therefore be considered as a one-phase Stefan problem. Ablation also occurs in other branches of physics, for example, in the melting or sublimation of a solid or laser drilling in metals and the cornea; see [22, 24, 40].

Goodman [13] applied the standard HBIM to this problem and compared results with a numerical solution of Landau [20], while Zien [45] applied an exponential

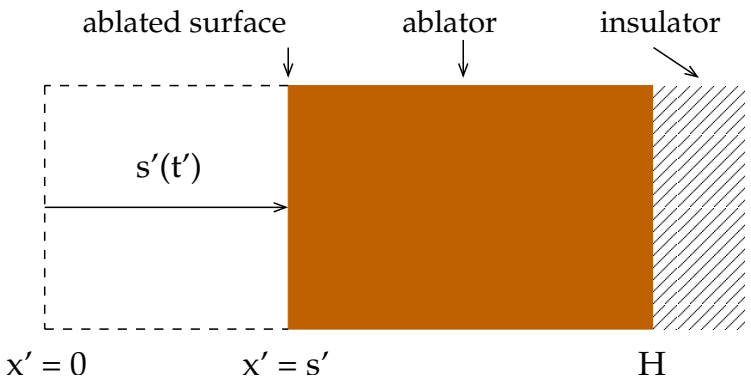

Fig. 7.1 *Typical ablator configuration.*

approximation. More recently, Braga and Mantelli [4, 5] have adapted the standard HBIM approach by assuming the temperature function is a polynomial of the form $v = a_0 + a_1(\delta - x)^n$, where the order n is determined by comparing the time ablation commences with standard exact analytical solutions for the preablation stage.

The typical problem configuration is shown in Figure 7.1. Initially the ablator is at a temperature $v'(x', 0) = V_0$ and the surface $x' = 0$ is subject to a heat flux Q, namely, $v'_{x'}(0, t') = -Q/k_s$. There follows a heating-up stage where heat penetrates the material and the surface $x' = 0$ reaches the ablation temperature V_a; subsequently material is removed at the ablating interface, $x' = s'(t')$, and we need only solve for the temperature in the solid which occupies $s'(t') \le x' \le H$. For simplicity we assume that the surface $x' = H'$ is insulated, so $v'_{x'}(H, t') = 0$. Since there is only a solid phase in this problem we use a slightly different nondimensionalization to previous sections and take the temperature scale $\Delta v = V_a - V_0$ and timescale $\tau = L^2/\kappa_s$.

For our purposes we can assume that the process occurs in three distinct stages. For $t \in [0, t_1]$ the boundary layer $0 < x < \delta(t)$ is heated, and this stage ends when $v(0, t) = 0$. In the second stage ablation occurs and the heat penetrates through the solid material until it reaches the end $x = H$ at $t = t_2$. During this stage there is always a region where the temperature is at the initial temperature, $v(x, t) = -1$. For $t \ge t_2$ the remaining material is all above the initial temperature and continues to heat up until it has all ablated. The equations governing the three stages are as follows.

- **Stage 1**, $t \in [0, t_1]$:

$$\frac{\partial^2 v}{\partial x^2} = \frac{\partial v}{\partial t}, \qquad v_x(0, t) = -\gamma_1, \quad v(\delta, t) = -1, \quad v_x(\delta, t) = 0, \tag{7.1}$$

  where $\gamma_1 = QL/(k_s \Delta v)$. If using a cubic approximation, the boundary conditions may be augmented by condition (6.12). The stage ends when $v(0, t_1) = 0$, which defines t_1.
- **Stage 2**, $t \in [t_1, t_2]$:

$$\frac{\partial^2 v}{\partial x^2} = \frac{\partial v}{\partial t}, \qquad v(s, t) = 0, \quad v(\delta, t) = -1, \quad v_x(\delta, t) = 0, \tag{7.2}$$

  and again $v_{xx}(\delta, t) = 0$ when using the cubic profile. The external heat input

now appears in the Stefan condition

$$\beta \frac{\mathrm{d}s}{\mathrm{d}t} = \gamma_1 + \left.\frac{\partial v}{\partial x}\right|_{x=s}, \tag{7.3}$$

where $\beta = L_m/(c_s \Delta v)$. This stage ends when $\delta(t_2) = H$.

- **Stage 3**, $t \in [t_2, t_3]$: The problem is now governed by the heat equation $v_t = v_{xx}$ and Stefan condition (7.3) subject to

$$v(s,t) = 0, \qquad v(H,t) = v_H(t), \qquad v_x(H,t) = 0, \tag{7.4}$$

where $v_H(t)$ represents the unknown temperature at $x = H$. The heat penetration depth has dropped out of the problem, but we must still determine two unknowns, namely, the position of the interface $s(t)$ and the temperature $v_H(t)$, where $v_H(t_2) = -1$ and t_3 is determined by $v_H(t_3) = 0$, or $s(t_3) = H$.

In Stage 1 the HBIM and ARIM formulations, respectively, are

$$\frac{\mathrm{d}}{\mathrm{d}t}\int_0^\delta v\,\mathrm{d}x + \frac{\mathrm{d}\delta}{\mathrm{d}t} = \gamma_1, \qquad \delta\frac{\mathrm{d}}{\mathrm{d}t}\int_0^\delta v\,\mathrm{d}x - \frac{\mathrm{d}}{\mathrm{d}t}\int_0^\delta xv\,\mathrm{d}x = -1 - v\big|_{x=0} + \gamma_1\delta,$$

with RIM found from ARIM by eliminating $\frac{\mathrm{d}}{\mathrm{d}t}\int_0^\delta v\,\mathrm{d}x$ using HBIM. The standard approach in the literature [4, 5, 24] is to use the profile $v = -1 + a_n(t)\big(1 - \frac{x}{\delta}\big)^n$ for some general exponent, $n \geq 2$. Applying the boundary conditions in (7.1) leads to

$$v = -1 + \frac{\gamma_1\delta}{n}\left(1 - \frac{x}{\delta}\right)^n. \tag{7.5}$$

Substituting v into the integral formulations and solving the resulting ODEs gives expressions for δ for HBIM, ARIM, and RIM. An analytical solution for Stage 1 is obtained by assuming a semi-infinite medium, then the temperature is [9, p. 75]

$$v = -1 + 2\gamma_1\left[\sqrt{\frac{t}{\pi}}e^{-x^2/(4t)} - \frac{x}{2}\mathrm{erfc}\frac{x}{2\sqrt{t}}\right], \tag{7.6}$$

with surface temperature $v(0,t) = -1 + 2\gamma_1\sqrt{t/\pi}$. Ablation starts when $v(0,t_1) = 0$, giving $t_1 = \pi/(4\gamma_1^2)$. The HBIM and RIM formulations lead to expressions of the same form for $v(0,t)$, with a different factor in the square root. Solving $v(0,t_1) = 0$ using profile (7.5) and expressions for δ gives

$$\text{HBIM:}\ \ t_1 = \frac{n}{\gamma_1^2(n+1)}, \quad \text{RIM:}\ \ t_1 = \frac{3n^2}{2\gamma_1^2(n+1)(n+2)},$$
$$\text{ARIM:}\ \ t_1 = \frac{(2n+1)n^2}{2\gamma_1^2(n^2-1)(n+2)}.$$

Following Mitchell and Myers [24], we use parameter values $Q = 2 \times 10^6\,\mathrm{W/m^2}$, $L = 2.5 \times 10^{-4}\,\mathrm{m}$, $k_s = 0.22\,\mathrm{W/mK}$, and $\Delta v = 560\,\mathrm{K}$. Then the error in t_1 predicted by the HBIM, RIM, and ARIM formulations, respectively, is 15.1%, 36.3%, 6.1% for the quadratic profile, and 4.5%, 14.1%, 0.27% for the cubic profile. In [24] a quartic profile is used (based on the small x or large time expansion of the exact solution); this leads to an error of 1.9% in t_1 for all three formulations. Braga and Mantelli [4, 5] replace the exponent 4 with a noninteger value, chosen to give an exact match

for t_1. For the standard HBIM this is $n = \pi/(4-\pi) \approx 3.66$, and for RIM a quadratic expression gives $n \approx 3.87$. In the case of ARIM, a solution cannot be found, but the resulting expression $\pi(n^2-1)(n+1) = 2(2n+1)n^2$ is minimized when $n \approx 2.95$.

Once ablation begins, since the boundary conditions change, it is possible to use a new approximating profile. Braga and Mantelli switch to the value $n = 7$ (to give a better match with numerical solutions). The main problem with this approach is that the choice of exponent is based on known solutions, either analytical or numerical, and there is no reason to suppose they are the best values for different boundary conditions where exact solutions cannot be found. Furthermore, in [24] it is shown that if the value of the exponent during ablation exceeds that chosen before ablation, then the solution becomes unphysical, in the sense that mass is added (rather than removed) for a brief period, causing $s'(t) < 0$. Their analysis concludes that the best postablation value is the same as the preablation one.

Therefore, in Stage 2 we consider a quartic profile for HBIM and RIM and a cubic profile for ARIM. Similar to (6.14), after satisfying the boundary conditions in (7.2), v is written in the form $v = -1 + (\delta - x)^n/(\delta - s)^n$ with $n = 4$ for HBIM and RIM and $n = 3$ for ARIM. The HBIM and ARIM integral formulations in this stage are

(7.7)
$$\frac{\mathrm{d}}{\mathrm{d}t}\int_s^\delta v\,\mathrm{d}x + \frac{\mathrm{d}\delta}{\mathrm{d}t} = -\frac{\partial v}{\partial x}\bigg|_{x=s}, \quad (\delta - s)\frac{\mathrm{d}\delta}{\mathrm{d}t} - s\frac{\mathrm{d}}{\mathrm{d}t}\int_s^\delta v\,\mathrm{d}x + \frac{\mathrm{d}}{\mathrm{d}t}\int_s^\delta xv\,\mathrm{d}x = -v\big|_{x=\delta},$$

with RIM again determined by combining the two. Substitution of v leads to ODEs involving s and δ, and these are coupled with the Stefan condition (7.3) and initial conditions $s(t_1) = 0$ and $\delta(t_1)$, which is found from Stage 1. As in section 6.2, we can compare these results to a numerical solution [26, 42]. We use parameter values $L_m = 2.326 \times 10^6\,\mathrm{J/Kg}$, $c_s = 1256\,\mathrm{J/Kg\,K}$, giving $\beta \approx 3.31$, and $H' = 1 \times 10^{-3}$, $L = 2.5 \times 10^{-4}$, giving $H = 4$ (since $H = H'/L$). Then the HBIM, RIM, and ARIM predictions for the end of this stage are $t_2 \approx 0.68$, 0.70, 1.05, respectively. Obviously, since $\delta(t)$ is a fictitious quantity introduced as part of the method, we cannot compare this time with the numerical solution. However, the percentage error in s at $t = 0.5$, well within the interval $[t_1, t_2]$, is 2.433%, 6.61%, 2.436% for HBIM, RIM, and ARIM, respectively.

In Stage 3 the profile which satisfies the boundary conditions in (7.4) is $v = v_H\big[1 - (H - x)^n/(H - s)^n\big]$. The HBIM, RIM, and ARIM formulations are similar to those in (7.7) from Stage 2, but with δ replaced by the constant boundary value H. These are again coupled with the Stefan condition (7.3). Stage 3 ends at time $t = t_3$ when $s(t_3) = H$, which is equivalent to $v_H(t_3) = 0$. The numerical solution predicts $t_3 = 4.24568$ and the percentage errors for t_3 are 0.01, 2.54, and 1.95 for the HBIM, RIM, and ARIM formulations, respectively. However, the errors grow with time so that, for example, at $t = 3$ the percentage errors are 2.17, 5.31, and 1.13 for the HBIM, RIM, and ARIM formulations, respectively.

7.2. Melting of a Subcooled Finite Material. Modeling a finite material heated at both ends requires dealing with a number of stages regardless of whether fixed temperature or cooling conditions are applied. However, all of these stages have been covered in previous sections. For example, consider a finite subcooled material of thickness L (which corresponds to unity in our nondimensional system). At $t = 0$ the temperature at either end is raised above the melting temperature, $u_1(0,t) = 1, u_2(1,t) = u_T$, where $u_T > 0$ and subscripts 1 and 2 correspond to the bottom and top layers, respectively. Both ends melt immediately and two separate boundary

layers form, where the end points are located at δ_1, δ_2. So initially we solve as if there were two separate semi-infinite regions. At some time the boundary layers meet, when $\delta_1 = \delta_2 = \delta$. In [35] this problem is tackled in modeling the melting of a block of ice. After the boundary layers meet they retain two approximating functions at either end but there is only one boundary layer thickness, δ, to solve for. A new unknown, the minimum temperature $v(\delta, t)$, is then introduced in the same manner as discussed for the ablation problem. The analysis subject to cooling conditions follows in the same manner.

A similar finite domain problem is the analysis of the contact melting process of a phase change material (PCM) in contact with a hot plate [34]. This leads to melting of the PCM, so a fluid layer forms between the two surfaces. The weight of the free solid acts to squeeze out the liquid and so the melt layer remains thin. Since the melt layer is flowing the authors use a quasi-steady approximation to the temperature in the thin liquid layer and the HBIM in the (initially) thicker solid layer. The analysis is carried out until the solid is completely melted. Excellent agreement is shown when the results are compared with experimental data.

7.3. Solidification from an Incoming Fluid. The solidification of a molten material sprayed onto a substrate that is maintained at a temperature below the melting temperature has numerous natural and industrial applications. Perhaps the most common example is when atmospheric water freezes on a structure. This has been studied in the context of icing on power transmission and generating equipment, aircraft, and seacraft. In an industrial setting solidification from a flowing liquid or a droplet spray is of interest in the casting of metals and spray forming and hydrate build-up in oil pipelines; see [7, 23].

In [23] this problem is studied in the context of ice build-up from supercooled droplets. In addition to the freezing front there is also a moving front due to the incoming spray (the two fronts do not always coincide). This is dealt with by the addition of a mass balance to the system of governing equations, and then the solution is a straightforward application of the techniques discussed so far. A quadratic HBIM is used and compared with a perturbation solution (up to second order) and a numerical solution. Melting times and the L_2 norm for the temperature predictions are evaluated. Excellent agreement between the numerical and approximate solutions is achieved and it is shown that the HBIM is often more accurate than the perturbation solution up to first order.

7.4. Incorporation of Source Terms. The incorporation of source terms into the heat equation leads to a straightforward extension of the integral methods. The only point to note is that when deriving the alternative Stefan condition, the source term must be accounted for. For example, if

$$u_t = u_{xx} + q(t), \tag{7.8}$$

and $u(\delta(t), t) = 1$, $u_x(\delta(t), t) = 0$ (see (6.12)), then instead of using $u_{xx}(\delta, t) = 0$ we find the new condition $u_{xx}(\delta, t) + q(t) = 0$. Antic and Hill [2] use this approach when modeling the temperature inside a grain silo. Kutluay, Wood, and Esen [19] include a source term in their model of a thermistor.

7.5. Time-Dependent Boundary Conditions. Here we see a significant drawback for the integral methods, namely, that if the temperature in the far field is constant (which we set to zero) and the temperature at the boundary then reaches zero, then due to the averaging inherent in the integral methods the temperature is

zero everywhere. Consider the problem with $u = u_x = u_{xx} = 0$ at $x = \delta$ and $u = u_a(t)$ at $x = 0$, where $u_a(t)$ is the varying ambient temperature. The cubic approximation gives

$$u = u_a \left(1 - \frac{x}{\delta}\right)^3. \tag{7.9}$$

If u_a is a monotonically decreasing function such that $u_a(0) > 0$ and $u_a(t_f) = 0$, then we expect heat to diffuse into the material. At any time $t > 0$ there will be some region where $u(x, t) > 0$, yet the approximation (7.9) shows that at time t_f, u is identically zero. For this reason studies such as those in [8, 18, 38] never carry out their analysis to a time where the boundary reaches zero. It was also noted in [13] that for boundary conditions of the form (2.5)(ii), with $h_s = 0$ and $Q \equiv Q(t)$, the HBIM is only useful for functions $Q(t)$ that are monotonically increasing or constant. However, this appears to be disproved in [30] where, using the technique of [31], the HBIM is applied a problem with $Q \propto 1/s(t)$.

Recently a new method has been developed for time-dependent boundary conditions, involving the product of a polynomial and logarithmic function [25]. For the cases examined in [25] the new profile appears to provide a much more accurate approximation to the temperature than previous HBIM solutions. In addition, it can accurately model solutions with a single moving peak in the temperature. However, this method has so far only been applied to thermal problems without a phase change.

Kinetic undercooling, where $u(s, t) = u_s(t) \propto s_t$, or surface tension effects, where $u(s, t) \propto \kappa$ and κ is the interface curvature (see [11, 44]), lead to a time-dependent temperature at the boundary $x = s(t)$. So far there are no examples in the literature of the application of heat balance methods to such problems. However, our preliminary calculations indicate that it should be possible to model these types of boundary condition with an HBIM, at least for small times, and that interesting behavior may be observed. For example, when applying $u(0, t) = 1$ and $u(s, t) = t$ we find that $s(t)$ initially increases to a maximum and then decreases. With kinetic undercooling the problem reduces to solving a second order equation for s rather than the standard first order equation.

8. Discussion and Conclusions. In this paper we have considered standard and refined HBIMs applied to a variety of phase change problems, including standard test cases with exact solutions and more interesting situations where analytical solutions cannot be found. Our aim is to provide an overview of popular approaches considered in recent literature, as well as giving new results which improve on previous work without complicating the formulation. Indeed, it is the simplicity of the HBIM that is responsible for its popularity. The refinements discussed here do not deviate from this premise and show a significant improvement in the results in almost all cases considered.

In the first part of the paper we examined the melting of a semi-infinite material at its solidus. In all cases shown the cubic approximation was more accurate than the standard quadratic, often by an order of magnitude. For the case of a fixed temperature boundary condition we found the exponential approximation gave slightly smaller errors than the cubic. However, this was the only example where it was the most accurate profile and in general the formulation is more complicated than with a polynomial, therefore we neglected it in later studies. From the results in section 5 it is clear that for this semi-infinite case, if u is prescribed on the $x = 0$ boundary, either as a constant or time-dependent condition, then the cubic RIM is the best method.

However, when the Robin condition or time-dependent flux is given, either the cubic HBIM or ARIM is now the most accurate.

In section 6 we examined the melting of a subcooled material. This time we found two cases, out of 23, where the standard quadratic HBIM was the most accurate. For the constant boundary condition, as shown in Tables 6.1 and 6.2, the cubic HBIM can be the the most accurate but it is not so clear cut as before; usually either the quadratic or cubic RIM formulations proved best. For the Robin condition, Tables 6.3 and 6.4 show that the RIM formulation is very seldom best and, in fact, since the errors for the quadratic profiles are significantly worse, it seems best to avoid RIM here. Then either the cubic HBIM or ARIM should be used. This is also shown to be true for the ablation problem; in Stages 2 and 3 the RIM profile has considerably larger errors. Hence, for all examples discussed here, the RIM profile should only be used when u and not $\frac{\partial u}{\partial x}$ is prescribed on the boundary.

The solutions presented in this study show that these approximate methods can provide accurate results, provided an appropriate choice is made for the method, HBIM or RIM, and order of the polynomial. Unfortunately, this choice appears to be both problem and parameter range-dependent. This highlights the classic problem of these methods, namely, how to choose the approximating function without knowledge of the exact or numerical solution. The general trend of our results suggests that a cubic is the best choice. This also has the advantage that there is only a single formulation, whereas the quadratic can have seven versions. However, recently a more definite answer to this question may have been found in terms of noninteger exponent polynomials, where the exponent is determined as part of the solution; see [31]. For example, in the premelting phase of the ablation problem discussed in section 7.1, the new method shows errors in the time to melting of 0.4% and 0.6% for the HBIM and RIM formulations, which is a significant improvement on the best results given in this paper for HBIM and RIM, namely, 4.5% and 14%, respectively.

A challenge still remaining for the HBIM and RIM community is how to deal with a time-dependent boundary condition which at some stage matches the far field temperature. The approximate methods currently predict a temperature equal to the far field everywhere. Consequently, studies with time-dependent boundary conditions all avoid this point. Our work here has perhaps shed light on the choice of approximating function or method, but not on how to deal with this issue. As mentioned in section 7.5, we have now successfully developed a new profile, combining a polynomial and logarithmic function, which can deal with a single moving peak in the temperature profile; see [25]. However, the application to Stefan problems still needs to be addressed.

REFERENCES

[1] J. A. Addison, S. D. Howison, and J. R. King, *Ray methods for free boundary problems*, Quart. Appl. Math., 64 (2006), pp. 41–59.

[2] A. Antic and J. M. Hill, *The double-diffusivity heat transfer model for grain stores incorporating microwave heating*, Appl. Math. Modelling, 27 (2003), pp. 629–647.

[3] G. E. Bell, *A refinement of the heat balance integral method applied to a melting problem*, Int. J. Heat Mass Trans., 21 (1978), pp. 1357–1362.

[4] W. F. Braga, M. B. H. Mantelli, and J. L. F. Azevedo, *Approximate analytical solution for one-dimensional ablation problem with time-variable heat flux*, in Proceedings of the 36th AIAA Thermophysics Conference, AIAA, 2003.

[5] W. F. Braga, M. B. H. Mantelli, and J. L. F. Azevedo, *Approximate analytical solution for one-dimensional finite ablation problem with constant time heat flux*, in Proceedings of the 37th AIAA Thermophysical Conference, AIAA, 2004.

[6] W. F. Braga, M. B. H. Mantelli, and J. L. F. Azevedo, *Analytical solution for one-dimensional semi-infinite heat transfer problem with convection boundary condition*, in Proceedings of the 38th AIAA Thermophysical Conference, AIAA, 2005.
[7] T. W. Brakel, J. P. F. Charpin, and T. G. Myers, *One dimensional ice growth due to incoming supercooled droplets impacting on a thin conducting substrate*, Int. J. Heat Mass Trans., 50 (2007), pp. 1694–1705.
[8] J. Caldwell and Y. Y. Kwan, *Numerical methods for one-dimensional Stefan problems*, Comm. Numer. Methods Engrg., 20 (2004), pp. 535–545.
[9] H. S. Carslaw and J. C. Jaeger, *Conduction of Heat in Solids*, 2nd ed., Oxford University Press, London, 1959.
[10] J. Crank, *Mathematics of Diffusion*, Clarendon Press, Oxford, 1975.
[11] J. D. Evans and J. R. King, *Asymptotic results for the Stefan problem with kinetic undercooling*, Quart. J. Mech. Appl. Math., 53 (2000), pp. 449–473.
[12] S. Fomin, V. Chugunov, and T. Hashida, *Analytical modelling of the formation temperature stabilization during the borehole shut-in period*, Geophys. J. Int., 155 (2003), pp. 468–478.
[13] T. R. Goodman, *The heat-balance integral and its application to problems involving a change of phase*, Trans. ASME, 80 (1958), pp. 335–342.
[14] T. R. Goodman, *Application of integral methods to transient nonlinear heat transfer*, Adv. Heat Trans., 1 (1964), pp. 51–122.
[15] T. R. Goodman and J. J. Shea, *The melting of finite slabs*, J. Appl. Mech., 27 (1960), pp. 16–27.
[16] J. M. Hill, *One-Dimensional Stefan Problems: An Introduction*, Longman Scientific and Technical, Harlow, UK, 1987.
[17] J. Hristov, *The heat-balance integral method by a parabolic profile with unspecified exponent: Analysis and benchmark exercises*, Thermal Sci., 13 (2009), pp. 27–48.
[18] S. Kutluay, A. R. Bahadir, and A. Ozdes, *The numerical solution of one-phase classical Stefan problem*, J. Comput. Appl. Math., 81 (1997), pp. 134–144.
[19] S. Kutluay, A. S. Wood, and A. Esen, *A heat balance integral solution of the thermistor problem with a modified electrical conductivity*, Appl. Math. Modelling, 30 (2006), pp. 386–394.
[20] H. G. Landau, *Heat conduction in a melting solid*, Quart. Appl. Math., 8 (1950), pp. 81–94.
[21] D. Langford, *The heat balance integral method*, Int. J. Heat Mass Trans., 16 (1973), pp. 2424–2428.
[22] W.-S. Lin, *Steady ablation on the surface of a two-layer composite*, Int. J. Heat Mass Trans., 48 (2005), pp. 5504–5519.
[23] S. L. Mitchell and T. G. Myers, *Approximate solution methods for one-dimensional solidification from an incoming fluid*, Appl. Math. Comput., 202 (2008), pp. 311–326.
[24] S. L. Mitchell and T. G. Myers, *A heat balance integral method for one-dimensional finite ablation*, AIAA J. Thermophys., 22 (2008), pp. 508–514.
[25] S. L. Mitchell and T. G. Myers, *Improving the accuracy of heat balance integral methods applied to thermal problems with time dependent boundary conditions*, Int. J. Heat Mass Trans., submitted (2009).
[26] S. L. Mitchell and M. Vynnycky, *Finite-difference methods with increased accuracy and correct initialization for one-dimensional Stefan problems*, Appl. Math. Comput., 215 (2009), pp. 1609–1621.
[27] F. Mosally, A. S. Wood, and A. Al-Fhaid, *An exponential heat balance integral method*, Appl. Math. Comput., 130 (2002), pp. 87–100.
[28] F. Mosally, A. S. Wood, and A. Al-Fhaid, *On the convergence of the heat balance integral method*, Appl. Math. Modelling, 29 (2005), pp. 903–912.
[29] T. G. Myers, *An extension to the Messinger model for aircraft icing*, AIAA J., 39 (2001), pp. 211–218.
[30] T.G. Myers, *Optimal exponent heat balance and refined integral methods applied to Stefan problems*, Int. J. Heat Mass Trans., to appear.
[31] T. G. Myers, *Optimizing the exponent in the heat balance and refined integral methods*, Int. Comm. Heat Mass Trans., 36 (2009), pp. 143–147.
[32] T. G. Myers and J. P. F. Charpin, *A mathematical model for atmospheric ice accretion and water flow on a cold surface*, Int. J. Heat Mass Trans., 47 (2004), pp. 5483–5500.
[33] T. G. Myers, J. P. F. Charpin, and S. J. Chapman, *The flow and solidification of a thin fluid film on an arbitrary three-dimensional surface*, Phys. Fluids, 14 (2002), pp. 2788–2803.
[34] T. G. Myers, S. L. Mitchell, and G. Muchatibaya, *Unsteady contact melting of a rectangular cross-section phase change material on a flat plate*, Phys. Fluids, 20 (2008), article 103101.

[35] T. G. Myers, S. L. Mitchell, G. Muchatibaya, and M. Y. Myers, *A cubic heat balance integral method for one-dimensional melting of a finite thickness layer*, Int. J. Heat Mass Trans., 50 (2007), pp. 5305–5317.
[36] J. R. Ockendon, S. D. Howison, A. A. Lacey, and A. Movchan, *Applied Partial Differential Equations*, Oxford University Press, Oxford, 1999.
[37] K. Pohlhausen, *Zur naherungsweisen Integration der Differentialgleichunger der Laminaren Grenzschicht*, Z. Math. Mech., 1 (1921), pp. 252–258.
[38] N. Sadoun, E.-K. Si-Ahmed, and P. Colinet, *On the refined integral method for the one-phase Stefan problem with time-dependent boundary conditions*, Appl. Math. Modelling, 30 (2006), pp. 531–544.
[39] H. Schlichting, *Boundary Layer Theory*, 8th ed., Springer, Berlin, 2000.
[40] A. B. Tayler, *Mathematical Models in Applied Mechanics*, Oxford University Press, Oxford, 2001.
[41] I. K. Volkov, V. A. Chugunov, and A. N. Salamatin, *Generalization of the method of integral correlations and its application to some heat transfer problems*, Geophys. J. Int., 41 (1988), pp. 1013–1029.
[42] M. Vynnycky, S. L. Mitchell, and J. Aberg, *On the treatment of infinitessimally thin regions in the modelling of solidification processes*, Internat. J. Numer. Methods Engrg., submitted (2009).
[43] A. S. Wood, *A new look at the heat balance integral method*, Appl. Math. Modelling, 25 (2001), pp. 815–824.
[44] B. Wu, S. W. McCue, P. Tillman, and J. M. Hill, *Single phase limit for melting nanoparticles*, Appl. Math. Modelling, 33 (2009), pp. 2349–2367.
[45] T.-F. Zien, *Integral solutions of ablation problems with time-dependent heat flux*, AIAA J., 16 (1978), pp. 1287–1295.
[46] T. F. Zien, *Application of heat balance integral method to droplet freezing in melting ablation*, in Proceedings of the 42nd AIAA Aerospace Sciences Meeting and Exhibit, AIAA, 2004.